BMC Genomics

RESEARCH

Open Access

Comparative mitogenomic analysis of subterranean and surface amphipods (Crustacea, Amphipoda) with special reference to the family Crangonyctidae

Joseph B. Benito[1†], Megan L. Porter[2†] and Matthew L. Niemiller[1*†]

Abstract

Mitochondrial genomes play important roles in studying genome evolution, phylogenetic analyses, and species identification. Amphipods (Class Malacostraca, Order Amphipoda) are one of the most ecologically diverse crustacean groups occurring in a diverse array of aquatic and terrestrial environments globally, from freshwater streams and lakes to groundwater aquifers and the deep sea, but we have a limited understanding of how habitat influences the molecular evolution of mitochondrial energy metabolism. Subterranean amphipods likely experience different evolutionary pressures on energy management compared to surface-dwelling taxa that generally encounter higher levels of predation and energy resources and live in more variable environments. In this study, we compared the mitogenomes, including the 13 protein-coding genes involved in the oxidative phosphorylation (OXPHOS) pathway, of surface and subterranean amphipods to uncover potentially different molecular signals of energy metabolism between surface and subterranean environments in this diverse crustacean group. We compared base composition, codon usage, gene order rearrangement, conducted comparative mitogenomic and phylogenomic analyses, and examined evolutionary signals of 35 amphipod mitogenomes representing 13 families, with an emphasis on Crangonyctidae. Mitogenome size, AT content, GC-skew, gene order, uncommon start codons, location of putative control region (CR), length of *rrnL* and intergenic spacers differed between surface and subterranean amphipods. Among crangonyctid amphipods, the spring-dwelling *Crangonyx forbesi* exhibited a unique gene order, a long *nad5* locus, longer *rrnL* and *rrnS* loci, and unconventional start codons. Evidence of directional selection was detected in several protein-encoding genes of the OXPHOS pathway in the mitogenomes of surface amphipods, while a signal of purifying selection was more prominent in subterranean species, which is consistent with the hypothesis that the mitogenome of surface-adapted species has evolved in response to a more energy demanding environment compared to subterranean amphipods. Overall, gene order, locations of non-coding regions, and base-substitution rates points to habitat as an important factor influencing the evolution of amphipod mitogenomes.

Keywords Cave, Crustaceans, Mitogenomes, OXPHOS, Selection, Stygobromus

[†]Joseph B. Benito, Megan L. Porter, and Matthew L. Niemiller contributed to conceptualization, data collection and curation, and manuscript writing and reviewing.

*Correspondence:
Matthew L. Niemiller
matthew.niemiller@uah.edu
Full list of author information is available at the end of the article

Introduction

Caves and other subterranean habitats, such as groundwater aquifers and superficial subterranean habitats (SSHs; [1]), represent some of the most challenging environments that exist on Earth. The primary characteristic of all subterranean habitats is the lack of light and associated photosynthesis [1, 2]. Though some subterranean ecosystems are supported by chemoautotrophic production by microbial communities [3, 4], chemoautotrophy rarely provides enough energy to support several trophic levels in most subterranean ecosystems [1, 5]. The primary source of energy input for many cave systems is the organic matter transferred from the surface hydrologically or by animals that frequently enter and exit caves [1, 6], which drive the structure and dynamics of subterranean communities [7–9]. Although most subterranean ecosystems are largely thought to be energy-limited [10], food availability can be highly variable both among and within cave systems [11, 12]. Previous studies have shown that many subterranean organisms living in such energy-limited habitats have undergone several physiological and metabolic adaptations to sustain themselves during extended food shortages [13, 14]. Among these troglomorphic traits, low metabolic rate is a key adaptation that occurs in both terrestrial and aquatic fauna of subterranean communities [15, 16].

Mitochondria are the primary sites of energy production in cells, generating ~ 95% of the adenosine triphosphate (ATP) required for everyday activities of life through oxidative phosphorylation [17–19]. The mitochondrial genome—mitogenome—encodes 13 essential proteins including two ATP synthases (*atp6* and *atp8*), three cytochrome oxidases (cox*1, cox2*, and *cox3*), seven NADPH reductases (*nad1*, *nad2*, *nad3*, *nad4*, *nad4l*, *nad5*, and *nad6*), and cytochrome *b* (*cytb*) subunits. All mitochondrial protein-coding genes (PCGs) play a vital role in the electron transport chain [20–22]. Due to the unique characteristics of mitochondria, including maternal inheritance, small genomic size, absence of introns, and their surplus availability in cells, the use of mitochondrial DNA (mtDNA) loci and mitogenomes has a long history in population genetics, phylogenetics, and molecular evolution studies [23–25]. Previous studies have demonstrated a close association between mitochondrial loci and energy metabolism [18, 26, 26, 27]. Although considered to largely evolve under purifying selection, there is growing evidence that mitogenomes may undergo episodes of directional selection in response to shifts in physiological or environmental pressures [28, 29] leading to improved metabolic performance under new environmental conditions [26, 30, 31]. For example, previous studies that investigated varying selective pressures acting on mitochondrial PCGs of insects and mammals have revealed significant positive selective constraints at several loci that have comparatively increased energy demands [18, 19, 32]. Similarly, other studies have shown the various adaptive mitochondrial responses of organisms surviving in extreme environments including the deep sea and Tibetan Plateau [29, 32, 33]. However, these adaptations can occur at different metabolic levels, not just mitochondrial metabolism [34, 35]. Thus, variation in mitogenomes of species inhabiting different environments may reflect only a small portion of these adaptive metabolic changes. Despite this limitation, previous studies have detected signals of directional selection in the mitogenomes of organisms dwelling in contrasting habitats with varying energy demands [36–38].

Amphipods (Class Malacostraca: Order Amphipoda) are one of the most ecologically diverse crustacean groups including over 10,000 species [39, 40], occurring in a diverse array of aquatic and even terrestrial environments globally, from aphotic groundwater aquifers and hadal depths to freshwater streams and lakes in temperate and tropical forests, among other habitats [41, 42]. Several studies have demonstrated the genetic basis of subterranean adaptation in several taxa, including dytiscid diving beetles [43], cave dwelling-cyprinid fishes [44, 45], anchialine cave shrimps [46], and cave isopods [47]. However, we still have a limited understanding of the mechanisms of subterranean adaptations in amphipods. Although physiological adaptations to challenging environments like cave and groundwater ecosystems have been well-studied in amphipods [13, 16], no studies to date have addressed the selective pressures and the molecular evolution mechanisms of mitochondrial energy metabolism loci in amphipods occupying caves and other subterranean habitats. Subterranean amphipods likely experience different evolutionary pressures on energy management due to lower levels of predation, lower food resources, and more stable environments compared to surface-dwelling taxa that generally experience higher levels of predation and energy resources [48, 49].

In this study, we compared the mitogenomes of surface and subterranean amphipods, including the 13 mitochondrial PCGs involved in the OXPHOS pathway to understand the potential molecular mechanisms of energy metabolism in this diverse crustacean group. Our aims were to test whether the mitochondrial PCGs showed evidence of adaptive evolution in subterranean environments in amphipods. We tested the hypothesis that the mitogenome of surface-adapted amphipods will be imprinted by mitogenomic adaptations to the energy demanding environment with greater signal of directional selection when compared to their subterranean counterparts. We compared base composition, codon

usage, gene order rearrangement, conducted comparative mitogenomic and phylogenomic analyses, and examined evolutionary signals using publicly available amphipod mitogenomes. In particular, we focused on the amphipod family Crangonyctidae, a diverse family that comprises species inhabiting a variety of surface and subterranean habitats and for which several mitogenomes have been sequenced and annotated recently [50, 51].

Materials and methods

We generated new mitogenomes recently for the following crangonyctid species: *Stygobromus pizzinii*, *S. tenuis potomacus*, *Bactrurus brachycaudus*, *Stygobromus allegheniensis*, and *Crangonyx forbesi* [51].

DNA extraction, library preparation, and sequencing

Whole genomic DNA from five crangonyctid species was isolated using the Qiagen DNA Easy Blood and Tissue kit and libraries were prepared using the Illumina TruSeq DNA Library Prep Kit (Illumina Inc., California). Libraries were then paired-end sequenced (2×150 bp) on an Illumina HiSeq 4000 platform at the Vincent J. Coates Genomics Sequencing Laboratory at the University of California, Berkeley. We assessed the quality of the raw reads using FastQC v0.11.5 [52], and the reads were trimmed and filtered using Trimmomatic v0.33 [53]. De-novo assembly was carried out using NOVOPlasty v2.6.3 assembler [54]. We then annotated the protein-coding genes, transfer RNAs (tRNAs), and ribosomal RNAs (rRNAs) for each of the five mitogenomes using the mitochondrial genome annotation web server MITOS [55]. The secondary structures of tRNAs were inferred using MITFI [56], a built-in module in MITOS. The locations of start and stop codons of protein coding genes were confirmed using NCBI ORFfinder [57] and by visual comparison to other published amphipod mitogenomes. The location of the control region was confirmed by the presence of a large intergenic spacer region with a string of thymines found immediately after *rrnS* and before *trnI*. We then downloaded from GenBank the annotated mitogenomes of 30 additional amphipod taxa that occupy aquatic habitats, including groundwater and springs, and three isopods that served as outgroups for comparative analyses.

Mitogenome analyses

Nucleotide composition, amino acid frequencies, and codon usage were calculated in PhyloSuite v1.1.15 [58, 59]. The web-based program CREx (http://pacosy.informatik.uni-leipzig.de/crex, [60]) was used to perform pair-wise comparison of the gene orders in the mitogenome to determine rearrangement events. CREx comparisons were based on common intervals, and it considers common rearrangement scenarios including transpositions, reversals, reverse transpositions, and tandem-duplication-random-losses (TDRLs). In addition, phylograms and gene orders were visualized in iTOL (https://itol.embl.de/, [61]) using files exported from PhyloSuite. AT and GC skew of entire mitogenomes and individual loci were calculated in PhyloSuite using the formulae: AT-skew = (A – T)/(A+T) and GC-skew = (G – C)/(G+C). Welch two sample t-tests were performed between the surface and subterranean amphipods for different mitogenomic features, including mitogenome length, AT content, AT and GC skew, and rRNA length using R [62]. Visualization of AT-skew, GC-skew, AT-content, and amino acid frequencies were generated in R.

Phylogenetic inference

The amino acid sequences of 13 PCGs of the five new mitogenomes [51], 30 previously published amphipod mitogenomes, and three isopod mitogenomes were aligned using MAFFT version 7 [63]. A total of 38 sequences with 350 positions in the alignment file were trimmed using Gblocks version 0.91b [64] to yield 255 positions (72%) in 6 selected blocks (parameters used: Supplementary Table S1). The alignment was partitioned by gene and then the best-fit partitioning strategy and evolutionary models for each partition were inferred using PartitionFinder v2.1.1 [65]; Supplementary Table S2). Phylogenetic relationships of the 35 amphipod mitogenomes and three isopod mitogenomes using the concatenated 13 PCG alignment were determined using Bayesian inference in MrBayes v3.2 [66]. The analyses contained two parallel runs with four chains each and were conducted for 5,000,000 generations (sampling every 100 generations). After dropping the first 25% "burn in" trees to ensure stationarity after examination of log-likelihood values for each Bayesian run using Tracer v1.7 [67], the remaining 37,500 sampled trees were used to estimate the consensus tree and the associated Bayesian posterior probabilities. All analyses were conducted within PhyloSuite.

Positive selection and selection pressure analyses of mitochondrial PCGs

We performed base-substitution analyses on entire mitogenomes as well as for each of the 13 PCGs individually to compare surface versus subterranean amphipod taxa. The non-synonymous to synonymous rate ratio (dN/dS or ω) for each PCG was estimated using the free-ratio model using the CodeML program implemented in PAML v4.8a [68]. The ω values were estimated for surface and subterranean species separately and visualized in R for comparison. To estimate the probability of

positively selected sites in each PCG across all amphipod species, we implemented site models (M1 and M2, M8a and M8), where ω was allowed to vary among sites [69]. To further investigate if some lineages and sites in particular lineages have undergone positive selection, we conducted maximum likelihood analyses on all PCG using the branch model and branch-site model in EasyCodeML v1.21, a visual tool for analysis of selection using CodeML [70].

To determine if all 13 PCG are free of functional constraints in subterranean lineages, we compared alternative branch selection models on each PCG tree. First, we tested a model (M0) where a single ω was estimated for all branches. This model was compared to a model (M1) with two ratios, a background ω for surface branches and a separate foreground ω for subterranean branches. In addition, we included a two-ratio model where ω was fixed at 1.0 in subterranean branches (M1fixed) to determine if estimates of ω differed from rates of neutral evolution and a model similar to the M1 model but where each subterranean lineage (*B. brachycaudus*, *B. jaraguensis*, *P. daviui*, and the clade containing *Stygobromus* and *Metacrangonyx*) was allowed to have a separate ω (M1a). We also examined a saturated model (M2) where each branch had its own ω. Akaike's information criterion (AIC) was used to compare models.

For both the branch and branch-site models, a likelihood ratio test (LRT) was conducted for each PCG to test whether ω was homogeneous across all branches. In the branch model, the null hypothesis assumes that the average ω values of branches of interest (ωF) is equal to that of other branches (ωB), whereas the alternative hypothesis assumes the opposite $\omega F \neq \omega B$. If the alternative hypothesis is supported and $\omega > 1$, the foreground lineage is under positive selection. The branch-site model allows ω to differ among codon sites in a foreground lineage when compared to background lineages. We implemented the branch-site model to identify sites on specific lineages regulated by positive selection. Selected sites were considered positively selected only if they passed a Bayes Empirical Bayes (BEB) analysis with a posterior probability of > 95%.

We performed selection pressure analyses on the concatenated 13 PCGs dataset aligned using the codon mode as well as on each PCG with the Bayesian topology (see Fig. 4) as the guidance tree using several approaches available from the Datamonkey Webserver [71]. First, we implemented aBSREL (Adaptive Branch-Site Random Effects Likelihood), an improved version of the commonly used "branch-site" models, to test if positive selection has occurred on a proportion of branches [72]. We implemented BUSTED (Branch-site Unrestricted Statistical Test for Episodic Diversification) to test for gene-wide (not site-specific) positive selection by querying if a gene has experienced positive selection in at least one site on at least one branch [73]. Finally, we implemented RELAX [74] to test whether the strength of selection has been relaxed or intensified along a specified set of test branches.

Results and discussion

We compared the mitogenomes for 35 surface and groundwater amphipods, including mitogenomes of one spring-dwelling and six groundwater species in the family Crangonyctidae by Aunins et al. [50] and Benito et al. [51], to determine whether subterranean species show evidence of adaptive evolution in subterranean habitats. Our study examined whether features of mitogenomes (e.g. base composition, codon usage, gene order) differed in relation to dominant habitat (surface vs. subterranean) and inferred the evolutionary forces potentially shaping mitogenome evolution in amphipods, with an emphasis on crangonyctid species.

Mitogenome length and content

Mitogenome sizes ranged from 14,113 to 18,424 bp for all amphipods and 14,661 to 15,469 bp for crangonyctid amphipods (Table 1). Mean mitogenome size of surface amphipods (15,770 ± 1206 bp; mean ± 1 standard deviation) was higher than that of the subterranean amphipods (14,716 ± 297 bp) (phylogenetic paired t-test: t = 0.586, df = 33, *p*-value = 0.562; Supplementary Figure S1). All crangonyctid amphipod mitogenomes possessed 13 PCGs, two rRNA genes, 22 tRNA genes, a control region, and intergenic spacers of varying number and lengths (Supplementary Figure S2, annotations of the genomes are presented in Supplementary Table S3) like other arthropods [75]. The length of the crangonyctid mitogenomes was similar to lengths reported for other amphipod families including Allocrangonyctidae, Caprellidae, Eulimnogammaridae, Gammaridae, Hadziidae, Lysianassidae, Metacrangonyctidae, Micruropodidae, Pallaseidae, Pontogeneiidae, Talitridae. Variation in mitogenome length within Crangonyctidae appears to be related to length variation in the *nad5, rrnL*, and *rrnS* loci, which were all notably longer in the *C. forbesi* mitogenome.

Base composition and AT- and GC-skews

Mitogenome AT% in all amphipods ranged from 62.2 to 76.9% (Table 1). Mean AT% of the subterranean amphipods (71.8 ± 3.6%) was higher than that of the surface amphipods (67.6 ± 3.4%) (phylogenetic paired t-test: t = 0.926, df = 33, *p*-value = 0.361). Mean AT% of all 13 PCG of the subterranean amphipods was significantly higher than that of the surface amphipods (Supplementary Figure S3a). Variation in AT% across

Table 1 Summary of mitogenomic characteristics, location, and habitat of subterranean and surface amphipods included for comparative mitogenome analyses

Accession number	Organism	Family	Full length (bp)	A + T(%)	ATskew	GCskew	Habitat/ locality	Surface vs. Subterranean	References
NC_026309	*Brachyuropus grewingkii*	Acanthogammaridae	17,118	62.2	0.003	-0.307	Lake Baikal, deep-water	Surface	Romanova et al. [76]
NC_019662	*Pseudoniphargus daviui*	Allocrangonyctidae	15,157	68.7	-0.002	-0.314	Spain, well	Subterranean	Bauzà-Ribot et al. [77]
NC_014492	*Caprella mutica*	Caprellidae	15,427	68.0	-0.023	-0.171	Shallow protected bodies of water in the Sea of Japan	Surface	Kilpert and Podsiadlowski [78]
NC_014687	*Caprella scaura*	Caprellidae	15,079	66.4	-0.015	-0.134	Western Indian Ocean	Surface	Ito et al. [79]
MN175619	*Bactrurus brachycaudus*	Crangonyctidae	14,661	63.9	0.004	-0.258	Fogelpole Cave, Monroe County, Illinois,	Subterranean	Benito et al. [51]
MN175623	*Crangonyx forbesi*	Crangonyctidae	15,469	67.9	0.061	-0.266	Unidentified spring, Monroe County, Illinois	Surface	Benito et al. [51]
MN175622	*Stygobromus allegheniensis*	Crangonyctidae	15,164	67.2	0.020	-0.261	Caskey Spring, Berkeley County, West Virginia	Subterranean	Benito et al. [51]
NC_030261	*Stygobromus indentatus*	Crangonyctidae	14,638	69.3	0.016	-0.270	Fort A.P. Hill, Caroline County, VA, seepage springs	Subterranean	Aunins et al. [50]
MN175620	*Stygobromus pizzinii*	Crangonyctidae	15,176	68.9	0.014	-0.248	Pimmit Run Seepage Spring, Arlington County, Virginia	Subterranean	Benito et al. [51]
KU869712	*Stygobromus tenuis potomacus*	Crangonyctidae	14,915	69.1	0.020	-0.275	Fort A.P. Hill, Caroline County, VA, seepage springs	Subterranean	Aunins et al. [50]
MN175621	*Stygobromus tenuis potomacus*	Crangonyctidae	14,712	69.1	0.022	-0.272	Pimmit Run Seepage Spring, Arlington County, Virginia	Subterranean	Benito et al. [51]
NC_033360	*Eulimnogammarus cyaneus*	Eulimnogammaridae	14,370	67.6	-0.019	-0.251	Lake Baikal, 0–3.5 m	Surface	Romanova et al. [76]
NC_023104	*Eulimnogammarus verrucosus*	Eulimnogammaridae	15,315	69.0	-0.008	-0.238	Lake Baikal, 0–12 m	Surface	Rivarola-Duarte et al. [80]
NC_025564	*Eulimnogammarus vittatus*	Eulimnogammaridae	15,534	67.4	-0.015	-0.222	Lake Baikal, 0–30 m	Surface	Romanova et al. [76]
NC_017760	*Gammarus duebeni*	Gammaridae	15,651	64.0	-0.016	-0.223	Intertidal zone of the North Atlantic region	Surface	Krebes and Bastrop [81]
NC_034937	*Gammarus fossarum*	Gammaridae	15,989	65.2	0.018	-0.261	Europe, freshwater	Surface	Macher et al. [82]
FR872382	*Bahadzia jaraguensis*	Hadziidae	14,657	69.7	0.037	-0.431	Dominican Rep, cave	Subterranean	Bauzà-Ribot et al. [77]

Table 1 (continued)

Accession number	Organism	Family	Full length (bp)	A + T(%)	ATskew	GCskew	Habitat/ locality	Surface vs. Subterranean	References
NC_013819	*Onisimus nanseni*	Lysianassidae	14,734	70.3	-0.004	-0.198	Below arctic pack ice near the Svalbard archipelago	Surface	Ki et al. [83]
NC_019654	*Metacrangonyx dominicanus*	Metacrangonyctidae	14,543	73.6	-0.016	-0.026	Dominican Rep, well	Subterranean	Bauzà-Ribot et al. [77]
NC_019655	*Metacrangonyx goulmimensis*	Metacrangonyctidae	14,507	69.7	-0.016	-0.028	Morocco, well	Subterranean	Bauzà-Ribot et al. [77]
NC_019656	*Metacrangonyx ilvanus*	Metacrangonyctidae	14,770	74.5	-0.014	-0.012	Italy, well	Subterranean	Bauzà-Ribot et al. [77]
NC_019658	*Metacrangonyx longicaudus*	Metacrangonyctidae	14,711	75.8	-0.014	-0.051	Morocco, well	Subterranean	Bauzà-Ribot et al. [77]
NC_013032	*Metacrangonyx longipes*	Metacrangonyctidae	14,113	76.1	-0.017	-0.035	Spain, Cala Figuera cave	Subterranean	Bauzà-Ribot et al. [77]
NC_019659	*Metacrangonyx panousei*	Metacrangonyctidae	14,478	76.1	-0.012	-0.051	Morocco, well	Subterranean	Bauzà-Ribot et al. [77]
NC_019660	*Metacrangonyx remyi*	Metacrangonyctidae	14,787	70.8	-0.014	0.017	Morocco, spring at maison forestière	Subterranean	Bauzà-Ribot et al. [77]
NC_019653	*Metacrangonyx repens*	Metacrangonyctidae	14,355	76.9	-0.025	-0.014	Spain, well	Subterranean	Bauzà-Ribot et al. [77]
HE860513	*Metacrangonyx sp. 1 MDMBR-2012*	Metacrangonyctidae	14,277	74.4	-0.019	-0.043	Not available	Subterranean	Bauzà-Ribot et al. [77]
HE860504	*Metacrangonyx sp. 3 ssp. 1 MDMBR-2012*	Metacrangonyctidae	14,644	75.1	-0.062	0.120	Not available	Subterranean	Bauzà-Ribot et al. [77]
HE860498	*Metacrangonyx sp. 4 MDMBR-2012*	Metacrangonyctidae	15,012	72.6	-0.009	0.005	Not available	Subterranean	Bauzà-Ribot et al. [77]
NC_019657	*Metacrangonyx spinicaudatus*	Metacrangonyctidae	15,037	74.8	0.010	-0.139	Morocco, well	Subterranean	Bauzà-Ribot et al. [77]
NC_033361	*Gmelinoides fasciatus*	Micruropodidae	18,114	65.9	-0.001	-0.303	Lake Baikal, 0–192 m	Surface	Romanova et al. [76]
NC_033362	*Pallaseopsis kessleri*	Pallaseidae	15,759	63.1	0.011	-0.182	Lake Baikal, 0–61 m	Surface	Romanova et al. [76]
JN827386	*Gondogeneia antarctica*	Pontogeneiidae	18,424	70.1	-0.006	-0.290	Coast of Antarctica, seawater	Surface	Shin et al. [84]
MG010370	*Platorchestia japonica*	Talitridae	14,780	72.5	0.015	-0.237	Pacific region esp. northeast Asia, terrestrial and supra-littoral habitats	Surface	Yang et al. [85]
MG010371	*Platorchestia parapacifica*	Talitridae	14,787	74.8	0.011	-0.253	Pacific region esp. northeast Asia, terrestrial and supra-littoral habitats	Surface	Yang et al. [85]

crangonyctid amphipod taxa ranged 63.9–69.3%, with a mean of 67.9 ± 1.93% (Table 1). Across loci, AT% ranged from a minimum of 60.0% at the *cox1* locus and a maximum of 75.5% at the *nad4l* locus (Fig. 1A). Variation in AT% across all PCGs combined ranged from 61.9% (*B. brachycaudus*) to 69.0% (*S. indentatus*). Genes encoded on the negative strand had a slightly higher AT-content values than those on the positive strand. The *nad6* locus showed the greatest variation in AT-content across species. *Bactrurus brachycaudus* displayed the outlier lower

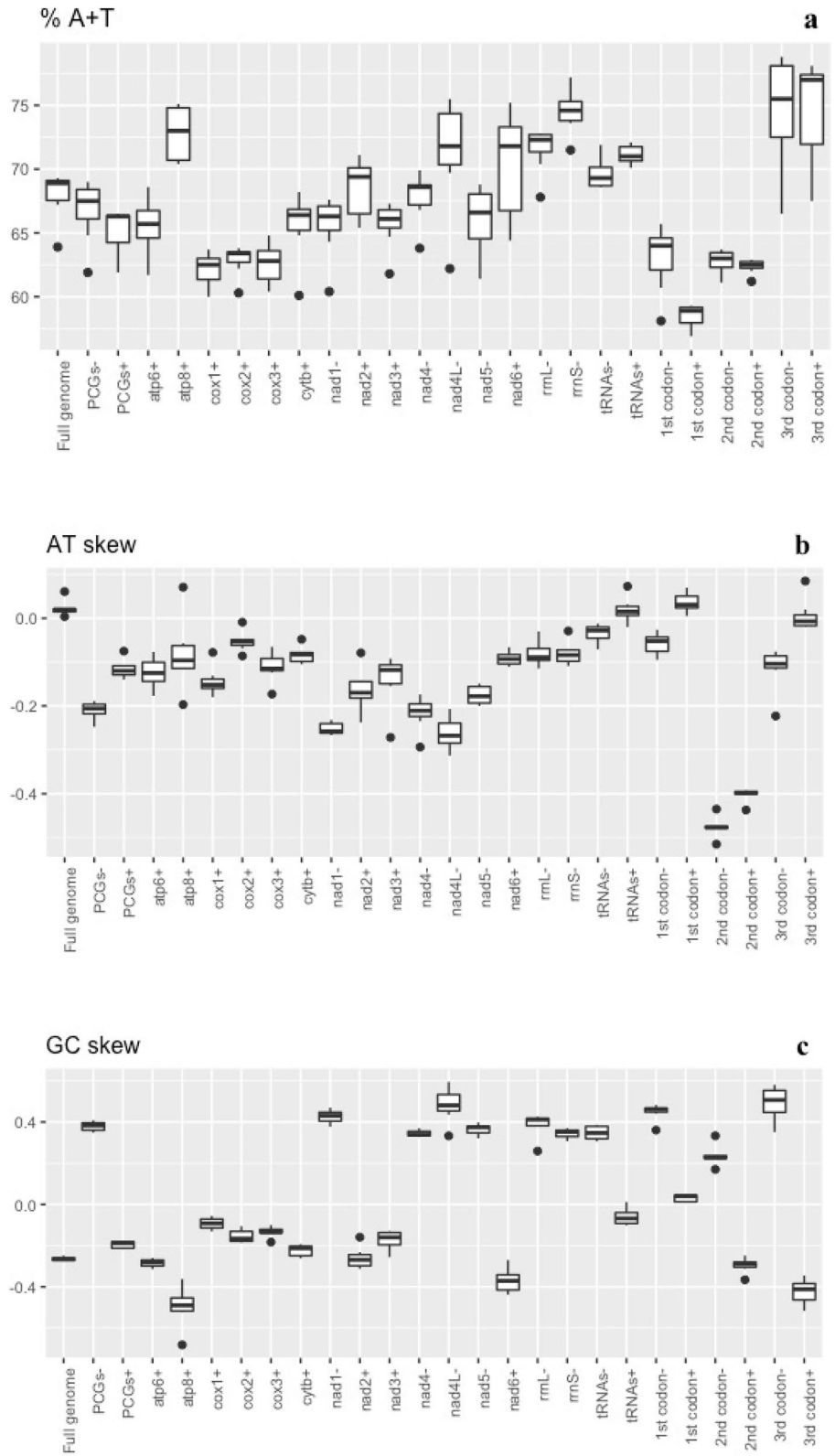

Fig. 1 Crangonyctidae mitochondrial nucleotide composition. Box plots showing values of nucleotide composition (A+T percentage) (**a**), AT-skew (**b**), and GC-skew (**c**) across mitogenomes, protein coding genes (PCG), and ribosomal (rRNA) and transfer ribosomal (tRNA) RNA. The same features are shown for each protein-coding gene and pooled by codon position and coding strand. Genes coded on the (-) strand are represented by a "-" sign and genes coded on the (+) strand are represented by "+" sign at the end of the gene label

AT% values for most of the PCG (Table 2; Fig. 1A). Similarly, *Bactrurus brachycaudus* had the lowest AT content (63.9%) among the crangonyctid mitogenomes, while all other mitogenomes had comparatively typical AT content reported for other arthropods [86, 87]. This could indicate that the evolution of the *B. brachycaudus* mitogenome has occurred under different evolutionary pressures (adaptive or non-adaptive) than other subterranean crangonyctids.

Mitogenome AT-skew in all amphipods ranged from −0.062 to -0.037. Mean AT-skew of the surface amphipods (0.001 ± 0.02) was positive and slightly higher than that of the subterranean amphipods (-0.004 ± 0.02) (phylogenetic paired t-test: t = 0.045, df = 33, *p*-value = 0.965). Mean AT-skew of four PCG (*cox1*, *cox2*, *nad2*, *nad3*) of surface amphipods was significantly higher than that of the subterranean amphipods, whereas the mean AT-skew of *nad4* of the subterranean amphipods was significantly higher than that of the surface amphipods (Supplementary Figure S3b). Among crangonyctid amphipods, mean AT-skew was 0.022 ± 0.02 (range 0.004 to 0.061), with all mitogenomes displaying positive skew. Mitogenome GC-skew ranged from −0.431 − 0.120. Mean GC-skew of the subterranean amphipods (-0.129 ± 0.15) was negative and higher than that of the surface amphipods (-0.236 ± 0.05) (phylogenetic paired t-test: t = 0.349, df = 33, *p*-value = 0.729). Mean GC-skew of seven PCG (*atp6*, *atp8*, *cox1*, *cox2*, *cox3*, *nad2*, *nad3*) of subterranean amphipods was significantly higher than that of the surface amphipods, whereas the mean GC-skew of *nad4* of the surface amphipods was significantly higher than that of the subterranean amphipods (Supplementary Figure S3c). Among crangonyctid amphipods, mean GC-skew was −0.264 ± 0.01 (range −0.275 to -0.248) with all mitogenomes displaying negative skew (Table 1). Strand asymmetry is commonly observed in mitogenomes [88, 89], however, at times it can hinder phylogenetic reconstruction and yield false phylogenetic artefacts especially when unrelated taxa display inverted skews [90, 91]. *Bactrurus brachycaudus* exhibited the lowest AT skew among the crangonyctid mitogenomes (0.004), while *S. tenuis* had the lowest GC skew (−0.275). Crangonyctid amphipod mitogenomes exhibited positive GC-skew values for genes encoded on the (-) strand and negative GC-skew for genes encoded on the (+) strand (Fig. 1C), whereas all PCGs exhibited negative AT-skew values (Fig. 1B). Except the six loci (*nad1, nad4, nad4L, nad5, rrnL*, and *rrnS*) which were encoded on the (-) strand, most PCG had negative GC skews. Such strand bias is typical for most mitochondrial genomes in metazoan [81, 83]. This is consistent with the hypothesis that strand asymmetry is caused by spontaneous deamination of bases in the leading strand during replication [88]. All other mitogenomes had comparatively typical AT and GC skew values like other amphipod species [76, 92]. The only outlier to this pattern was the positive GC skew value of tRNAs encoded on the (+) strand of B. *brachycaudus* (0.012). In general, crangonyctid mitogenomes exhibited relatively consistent skews.

Rearrangements of mitochondrial genome

Comparisons of crangonyctid mitogenomes revealed at least six conserved gene blocks (Fig. 2B). The gene orders in subterranean species (genera *Stygobromus* and *Bactrurus*) are identical except for the transposition of tRNA-*G,W*. However, a few unique gene order arrangements were observed in the spring-dwelling *C. forbesi*. The gene order of *C. forbesi* differs from the four subterranean species in the locations of the conserved gene blocks (tRNA-*H*-nad4-*nad4l* and *nad6-cytb*-tRNA-*S2* and tRNA-*L1-rrnL* and *rrnS*-tRNA-*I* and tRNA-*Y,Q*), seven tRNAs (*P,T,M,V,G,C*, and *W*), and two protein-coding loci: *nad1* and *nad2*. Compared to the conserved mitogenome gene orders of other crangonyctid mitogenomes, another unique feature in the rearranged *C. forbesi* mitogenome was the presence of at least two long (~ 50 and 70 bp) non-coding regions (Supplementary Table S3). The locations of rRNA genes in all crangonyctid mitogenomes are mostly similar compared to the pancrustacean ground pattern except for *C. forbesi* where the rRNA genes had altered positions (Fig. 2A and B). Rearrangements in the mitogenome is common especially when it involves only tRNA-coding genes [93]. In case of ribosomal RNA genes or PCGs, rearrangements occur much less frequently, and they are commonly referred to as major rearrangements, as they might potentially affect the differential regulation of replication and transcription of mitogenomes [94].

CREx analysis indicated that transpositions and TDRL may have been responsible for the evolution of mitogenomes in crangonyctid amphipods. Two transpositions of tRNA-*R,N,S1,E* and two steps of TDRL from the ancestral pan-crustacean pattern were needed to generate the gene order observed in *Stygobromus* species. In addition to the same two transpositions, one TDRL, and a transposition within a second TDRL from the ancestral pattern were required to generate the gene order in *Bactrurus*. However, four different transpositions (tRNA-*N,S1*, tRNA-*T,P*, tRNA-*W,C* and gene block tRNA-*H*-*nad4*-*nad4L*-tRNA-*P,T*-*nad6*-*cytb*-tRNA-*S2*) and three steps of TDRL from the ancestral pattern were needed to generate the gene order observed in *C. forbesi* (Supplementary Figure S4).

Similar to *C. forbesi*, other surface amphipods including *Gmelinoides fasciatus* (Micruropodidae) and *Onisimus nanseni* (Lysianassidae) exhibited a highly

Table 2 Comparison of mitogenomic characteristics of 35 amphipods discussed in this study

Species	Accession number	PCGs				rRNAs				tRNAs			
		Length (bp)	A + T (%)	AT skew	GC skew	Length (bp)	A + T (%)	AT skew	GC skew	Length (bp)	A + T (%)	AT skew	GC skew
Bactrurus brachycaudus	MN175619	11,028	61.9	-0.177	0.090	1705	69.3	-0.030	0.374	1275	69.8	-0.028	0.192
Bahadzia jaraguensis	FR872382	11,073	68.7	-0.145	0.109	1788	72.4	-0.076	0.477	1332	71.7	0.005	0.174
Brachyuropus grewingkii	NC_026309	11,046	60.2	-0.156	0.067	1608	66.3	-0.074	0.383	1304	65.4	0.012	0.137
Caprella mutica	NC_014492	10,989	66.2	-0.195	0.019	1742	72.2	-0.050	0.176	1338	71.8	0.011	0.116
Caprella scaura	NC_014687	10,986	64.6	-0.190	0.048	1739	71.7	-0.024	0.149	1318	70.4	-0.015	0.149
Crangonyx forbesi	MN175623	11,304	65.9	-0.162	0.065	1785	73.1	-0.072	0.297	1317	71.5	0.001	0.177
Eulimnogammarus cyaneus	NC_033360	11,043	67.0	-0.139	0.092	1607	71.8	-0.095	0.377	1300	66.8	0.026	0.132
Eulimnogammarus verrucosus	NC_023104	11,019	68.0	-0.141	0.097	1602	69.6	-0.072	0.348	1335	67.1	-0.002	0.123
Eulimnogammarus vittatus	NC_025564	11,046	65.7	-0.144	0.072	1606	71.3	-0.072	0.341	1373	66.9	0.020	0.131
Gammarus duebeni	NC_017760	11,019	61.6	-0.165	0.074	1623	65.0	-0.037	0.345	1319	63.6	0.029	0.124
Gammarus fossarum	NC_034937	11,031	62.7	-0.163	0.073	2614	72.4	-0.022	0.269	1302	66.4	0.011	0.136
Gmelinoides fasciatus	NC_033361	11,091	63.5	-0.141	0.081	1594	69.0	-0.031	0.332	1348	66.2	0.025	0.147
Gondogeneia antarctica	JN827386	10,794	67.3	-0.158	0.088	800	70.3	-0.007	-0.261	1364	70.0	0.019	0.107
Metacrangonyx dominicanus	NC_019654	11,064	72.1	-0.189	0.075	1691	77.6	-0.036	0.232	1301	77.7	0.039	0.177
Metacrangonyx goulmimensis	NC_019655	11,067	67.7	-0.175	0.034	1755	75.2	-0.015	0.292	1298	74.8	0.055	0.145
Metacrangonyx ilvanus	NC_019656	11,064	72.9	-0.181	0.057	1750	78.1	-0.026	0.260	1306	77.2	0.029	0.211
Metacrangonyx longicaudus	NC_019658	11,055	74.8	-0.170	0.070	1757	78.5	-0.002	0.270	1309	77.4	0.017	0.209
Metacrangonyx longipes	NC_013032	11,070	75.4	-0.170	0.082	1832	78.8	-0.026	0.263	1287	78.2	0.047	0.204
Metacrangonyx panousei	NC_019659	11,025	75.2	-0.174	0.086	1751	78.4	-0.031	0.314	1349	76.5	0.073	0.188
Metacrangonyx remyi	NC_019660	11,055	68.6	-0.184	0.044	1728	73.6	0.002	0.189	1296	74.7	0.039	0.198
Metacrangonyx repens	NC_019653	11,064	76.0	-0.172	0.101	1752	79.3	-0.022	0.280	1299	79.1	0.057	0.196
Metacrangonyx sp. 1 MDMBR-2012	HE860513	11,085	73.4	-0.172	0.077	1758	77.4	-0.011	0.315	1305	76.7	0.040	0.191
Metacrangonyx sp. 3 ssp. 1 MDMBR-2012	HE860504	11,076	73.9	-0.167	0.068	1752	78.2	-0.015	0.139	1303	76.8	0.045	0.208
Metacrangonyx sp. 4 MDMBR-2012	HE860498	11,076	70.3	-0.190	0.054	1731	75.2	-0.024	0.252	1298	75.4	0.021	0.207
Metacrangonyx spinicaudatus	NC_019657	11,067	73.3	-0.155	0.045	1749	77.4	-0.013	0.352	1310	78.0	0.032	0.161
Onisimus nanseni	NC_013819	11,046	69.0	-0.170	0.102	1840	76.3	-0.009	0.286	1396	73.4	0.024	0.137
Pallaseopsis kessleri	NC_033362	11,028	61.2	-0.147	0.027	1597	64.9	-0.071	0.241	1302	67.8	0.009	0.114
Platorchestia japonica	MG010370	11,043	70.9	-0.201	0.109	1610	75.4	-0.069	0.338	1342	76.9	0.027	0.183
Platorchestia parapacifica	MG010371	11,043	73.6	-0.185	0.115	1609	77.1	-0.066	0.330	1330	76.9	0.022	0.195
Pseudoniphargus daviui	NC_019662	10,998	66.6	-0.176	0.097	1710	73.8	-0.076	0.433	1307	70.2	0.031	0.139
Stygobromus allegheniensis	MN175622	10,980	64.6	-0.178	0.106	1722	71.9	-0.112	0.390	1303	69.4	0.004	0.119
Stygobromus indentatus	NC_030261	11,100	67.7	-0.149	0.085	1704	74.5	-0.081	0.356	1304	71.5	-0.016	0.170

Table 2 (continued)

Species	Accession number	PCGs				rRNAs				tRNAs			
		Length (bp)	A + T (%)	AT skew	GC skew	Length (bp)	A + T (%)	AT skew	GC skew	Length (bp)	A + T (%)	AT skew	GC skew
Stygobromus pizzinii	MN175620	11,088	66.9	-0.159	0.086	1715	73.3	-0.086	0.386	1309	70.3	-0.003	0.112
Stygobromus tenuis potomacus	KU869712	11,112	67.4	-0.154	0.099	1717	73.2	-0.095	0.383	1300	70.2	-0.005	0.109
Stygobromus tenuis potomacus	MN175621	11,091	67.4	-0.163	0.111	1715	74.1	-0.088	0.405	1306	70.2	-0.007	0.129

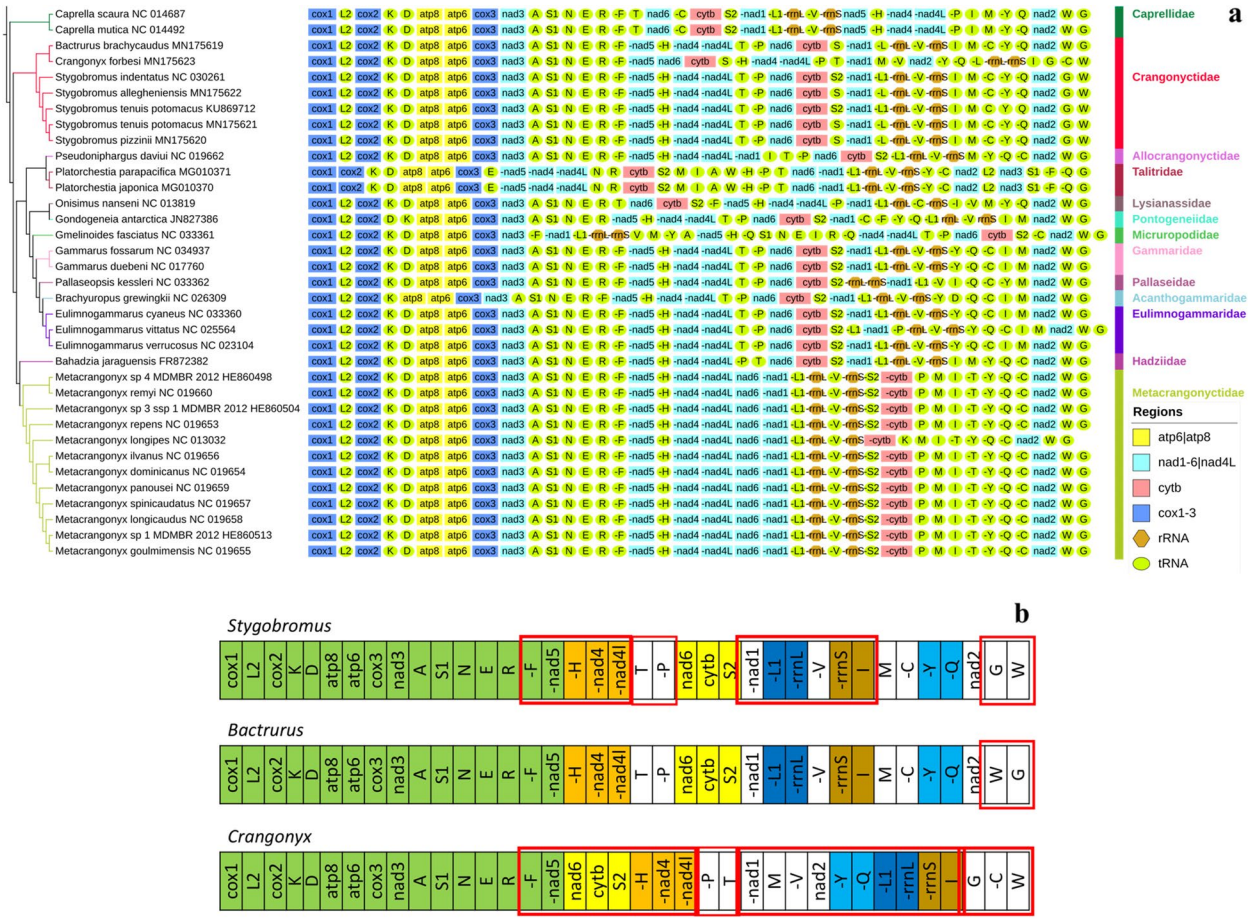

Fig. 2 Mitochondrial phylogenomics and gene orders: (**a**) Bayesian phylogram inferred using amino acid sequences of all mitochondrial PCGs (left) and gene orders (right). Three isopod outgroups are not shown. GenBank accession numbers are included as suffix next to the species names; (**b**) gene orders of mitochondrial genomes in three genera of crangonyctid amphipods, including *Stygobromus*, *Bactrurus*, and *Crangonyx*. Conserved gene clusters are indicated by different colors and gene rearrangements are highlighted by red border lines

rearranged gene order. Other surface amphipods that exhibited a moderate to highly rearranged gene order include *Gondogeneia antarctica* (Pontogeneiidae), *Platorchestia parapacifica* and *P. japonica* (Talitridae), *Pallaseopsis kessleri* (Pallaseidae), and the two basal amphipods *Caprella scaura* and *C. mutica* (Caprellidae) (Fig. 2A). Interestingly, a subterranean amphipod *Pseudoniphargus daviui* (Allocrangonyctidae) also exhibited a moderate rearranged gene order. The stark contrast between the highly conserved gene order in most subterranean amphipods and the highly volatile gene order in many of the surface amphipods may support the hypothesis that evolution of mitogenomic architecture could be highly discontinuous. A long period of inactivity in gene order and content could have been interspersed by a rearrangement event, this destabilized mitogenome is much more likely to undergo subsequent accelerated rate of mitogenomic rearrangements [95]. Thus, it is appealing to examine mitogenomes of surface amphipod families represented by just a single taxon in our dataset.

Codon usage and amino acid frequencies

In addition to the regular start codons (ATA and ATG) and uncommon start codons (ATT, ATC, TTG, and GTG), surface amphipods, particularly *Caprella scaura*, possessed one rare start codon CTG, whereas subterranean amphipods possessed three rare start codons including CTG, TTT, and AAT to initiate the mitochondrial PCGs (Supplementary Table S4). Codon usage analysis of the five crangonyctid amphipods mitogenomes identified the existence of all codon types typical for any invertebrate mitogenome. In addition to the regular start codons (ATA and ATG), uncommon start codons (ATT, ATC, TTG, and GTG) were also present to initiate the mitochondrial PCG. Such unusual start codons have been reported previously in other arthropods [96, 97]. A few PCG in the crangonyctid mitogenomes possessed

truncated or incomplete stop codons (TA- and T–) that have been described in other crustaceans (Supplementary Table S3). These are presumably completed after a post-transcriptional polyadenylation [98–100]. Among the crangonyctid mitogenomes, the most frequently used codons are TTA (Leu2; 5.64–8.49%) and TTT (Phe; 5.94–6.78%). Other frequently used codons include ATT (Ile; 4.92–6.85%) and ATA (Met; 4.13–5.34%) (Supplementary Table S5). These four codons are also among the most abundant in non-crangonyctid amphipods included in this study. This bias towards the AT-rich codons is quite typical for arthropods [101]. Among crangonyctid amphipod mitogenomes, relative synonymous codon usage (RSCU) values, which is the measure of the extent that synonymous codons depart from random usage, showed a high prevalence of A or T nucleotides at third codon positions (Fig. 3). This trend was also observed in other subterranean and surface amphipods. This positive

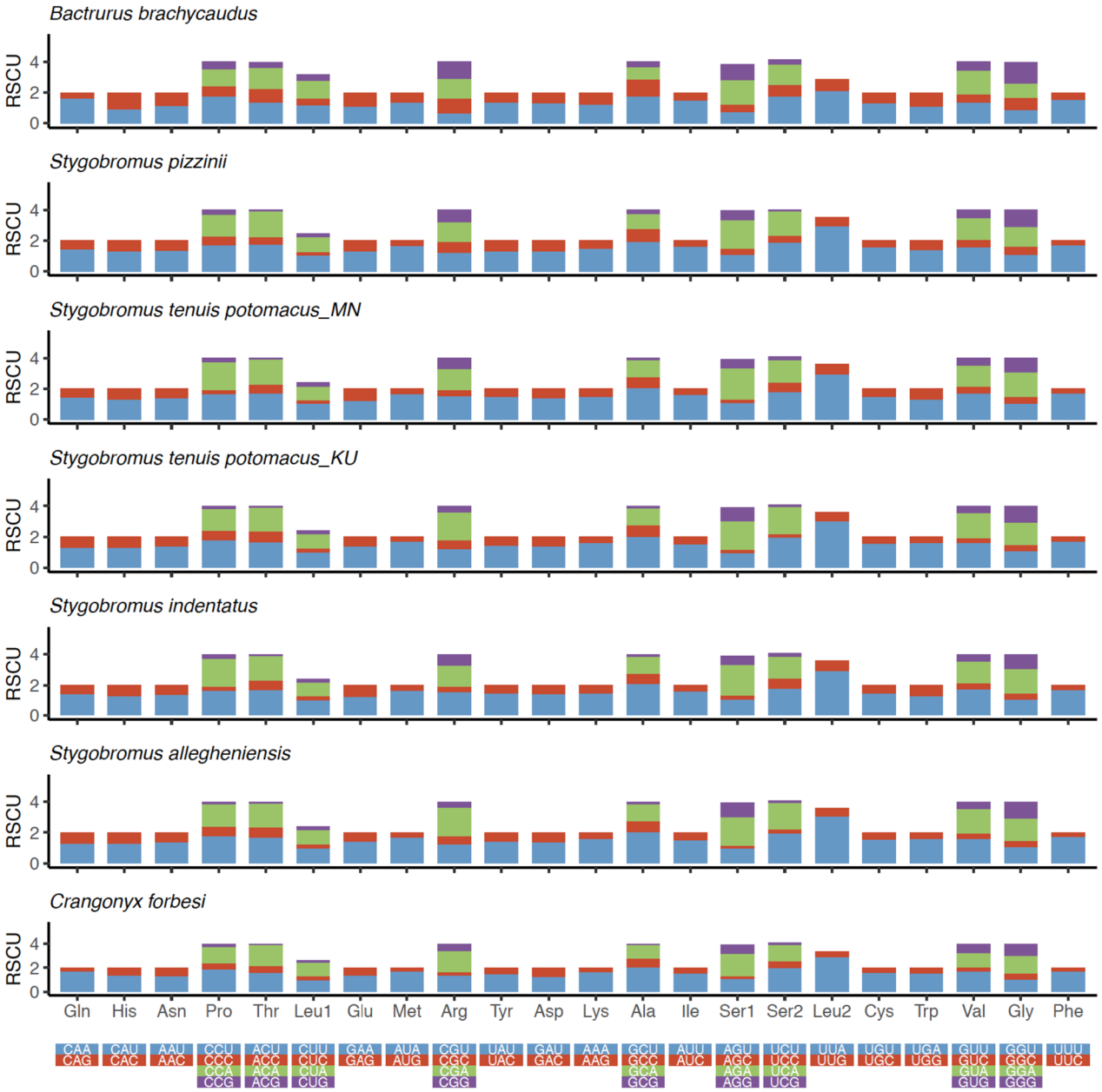

Fig. 3 The relative synonymous codon usage (RSCU) of the mitogenome of all crangonyctid amphipods. The RSCU value are provided on the Y-axis and the codon families are provided on the X-axis

correlation between RSCU and AT content at third codon positions has been reported in mitochondrial genomes of the abalone and oyster [102–104].

In PCGs, the second copy of leucine (8.86–10.01%) and cysteine (0.95–1.17%) are the most and the least used amino acids, respectively. Amino acid frequency analysis of both surface and subterranean amphipods indicated that five amino acids (leucine, phenylalanine, isoleucine, methonine, and valine) account for more than half of the total amino acid composition and exhibited greater variation among species (Supplementary Figure S5; Supplementary Table S6).

Transfer RNA genes

All 22 tRNA genes were identified in the mitogenomes of crangonyctid amphipods. However, the locations of tRNA genes were highly variable among these mitogenomes, and they also displayed altered positions relative to the pancrustacean ground pattern (Fig. 2; Supplementary Figure S3). The secondary structures of all mitogenome-encoded tRNAs belonging to crangonyctid amphipods were predicted and ranged in length from 50 to 66 bp. Most of the tRNAs displayed the regular cloverleaf structures, however, a few displayed aberrant structures. The tRNA-Ser1 (UCU) lacked the DHU arm in all crangonyctid species. Similarly, the tRNA-Ser2 (UGA) lacked the DHU arm in all crangonyctid species except *S. allegheniensis* where tRNA-Ser2 (UGA) possessed the DHU arm. The DHU arm was also missing in the tRNA-Cys and tRNA-Arg of *B. brachycaudus* and tRNA-Arg of *C. forbesi*. The tRNA-Gln lacked the TψC arm in all crangonyctid species except *C. forbesi* where tRNA-Gln possessed the TψC arm. In addition to lacking the TψC arm, tRNA-Gln of *B. brachycaudus* lacked the acceptor stem as well (Supplementary Figure S6). The presence of aberrant structures in tRNAs have been observed in several other crustaceans and invertebrates [79, 105–107], which may be the result of replication slippage [108] or selection towards minimization of the mitogenome [109].

Ribosomal RNA genes

The length of *rrnL* genes in all amphipods ranged 976–1,137 bp and that of *rrnS* genes ranged 618–1,631 bp. *rrnL* length of the subterranean amphipods (1,055 ± 26 bp) was higher than that of the surface amphipods (1005 ± 46 bp) (phylogenetic paired t-test: t = 0.921, df = 33, *p*-value = 0.364). *rrnS* length of the surface amphipods (738 ± 258 bp) was higher than that of the subterranean amphipods (684 ± 16 bp) (phylogenetic paired t-test: t = -0.558, df = 33, *p*-value = 0.581). The length of *rrnL* genes in crangonyctid amphipods ranged 1,034–1,090 bp and that of *rrnS* genes ranged 671–695 bp. The length of rRNA genes in crangonyctid amphipods was similar to that of other amphipod mitogenomes except *C. forbesi*, which had long overhangs (~50 bp and ~25 bp) on the 5' end of the *rrnL* and *rrnS* genes, respectively. AT content ranged 67.8–72.8% in the *rrnL* genes and 71.5–77.2% in the *rrnS* genes of crangonyctid species, respectively. GC-skew values for rRNA genes were positive (0.259 to 0.426) and comparable to that of PCGs encoded on the (-) strand (Supplementary Table S7).

Control region and intergenic spacers

In the mitogenome of *S. pizzinii* the putative control region (CR) was identified as a 1,021 bp sequence between the *rrnS* gene and the *trnl-trnM-trnC-trnY-trnQ-nad2* gene cluster. Similarly, CR was observed in the other crangonyctid mitogenomes, including *S. tenuis* (556 bp), *S. allegheniensis* (991 bp), *B. brachycaudus* (531 bp), *S. indentatus* (535 bp), and *S. tenuis potomacus* (773 bp). The CR was similarly located between the *rrnS* and *nad2* genes in some of the other mitogenomes of non-crangonyctid amphipods, including *G. duebeni* [81], *O. nanseni* [83], G. *antarctica* [84], P. *daviui* [77], and for the pancrustacean ground pattern. However, the adjacent tRNA genes were often different. In *G. fasciatus*, the CR region was located between the *rrnS* and *nad5* genes [76]. In contrast, a control region 843 bp was observed in *C. forbesi* which is located between the *nad1* and *trnM-trnV-nad2* gene cluster and separated by few intergenic spacers was identified as the CR (Supplementary Figure S2; Supplementary Table S3). The only other surface amphipod that had a similar CR location to *C. forbesi* was *P. kessleri* with the CR located between *nad1* and *nad2* genes, although the adjacent tRNA genes were different [76]. Thus, the variable location of the CR in *C. forbesi* was in concordance with a few surface amphipods, while the subterranean amphipods mostly followed the universal pattern between *rrnS* and *nad2* genes.

The non-coding regions or intergenic spacers identified in the crangonyctid mitogenomes varied in number and length. The number of intergenic spacers ranged from 7 to 17 and their lengths ranged from 1 to 99 bp (mean 13.0 bp ± 18.6). Two crangonyctid mitogenomes (*S. allegheniensis* and *C. forbesi*) possessed the largest intergenic spacers (a total of 220 and 249 bp, respectively; Supplementary Table S3). Among the non-crangonyctid amphipods, *G. fasciatus* and *G. antarctica* possessed relatively large non-coding intergenic spacers (a total of 3,863 bp and 4,354 bp, respectively; [76, 84].

Phylogenetic inference

The phylogenetic analyses of the 13 concatenated PCG from 35 amphipod species using Bayesian Inference (BI) resulted in a well-supported phylogeny, with the crangonyctid species forming a well-supported monophyletic

group (Fig. 4). Within Crangonyctidae, *Stygobromus* species formed a monophyletic group sister to *Bactrurus* + *Crangonyx*; however, few crangonyctid taxa were included in our analysis. A previous study based on the *cox1* gene found that *Stygobromus* was not monophyletic, but several relationships had low support [110]. Likewise, *Stygobromus* was recovered as polyphyletic in a multilocus concatenated phylogenetic analysis of the Crangonyctidae by Copilaş-Ciocianu et al. [111]. In addition, several well-supported clades were recovered within Crangonyctidae but relationships among these clades had low support. Other past studies have not supported monophyly of the widespread genera (i.e., *Crangonyx*, *Stygobromus*, and *Synurella*) in the family based on either morphological [112] or molecular data [113, 114]. A comprehensive phylogenomic study with robust taxonomic sampling is greatly needed to better elucidate evolutionary relationships and test biogeographic and ecological hypotheses regarding the origin and diversification of this diverse family of subterranean and surface-dwelling amphipods.

Selection in PCGs

Most of the energy required for active movement to escape predation and meet energy demands is supplied by the mitochondrial electron transport chain [99, 100. Mitochondrial genes encode for all of the protein complexes related to oxidative phosphorylation except for succinate dehydrogenase (complex II) [115–117]. Because of their importance in oxidative phosphorylation during cellular respiration, it is unsurprising that many studies have shown evidence of purifying (negative) selection in mitochondrial PCG [29, 118, 119]. While we found strong evidence for purifying selection in amphipod mitochondrial PCGs in our selection analyses, we also found signatures of positive selection in a few of the mitochondrial PCGs in the surface amphipods.

Using a free-ratio model (M2; [27]), we calculated the ω values for the 13 PCGs for the terminal branches to estimate the strength of selection between different primary habitats (i.e., subterranean vs. surface). The *cox2* locus significantly differed in ω values between the amphipods of the two habitat types ($p = 0.020$), with higher ω values for the surface amphipods. Similarly, *cox1* and *cox3* genes

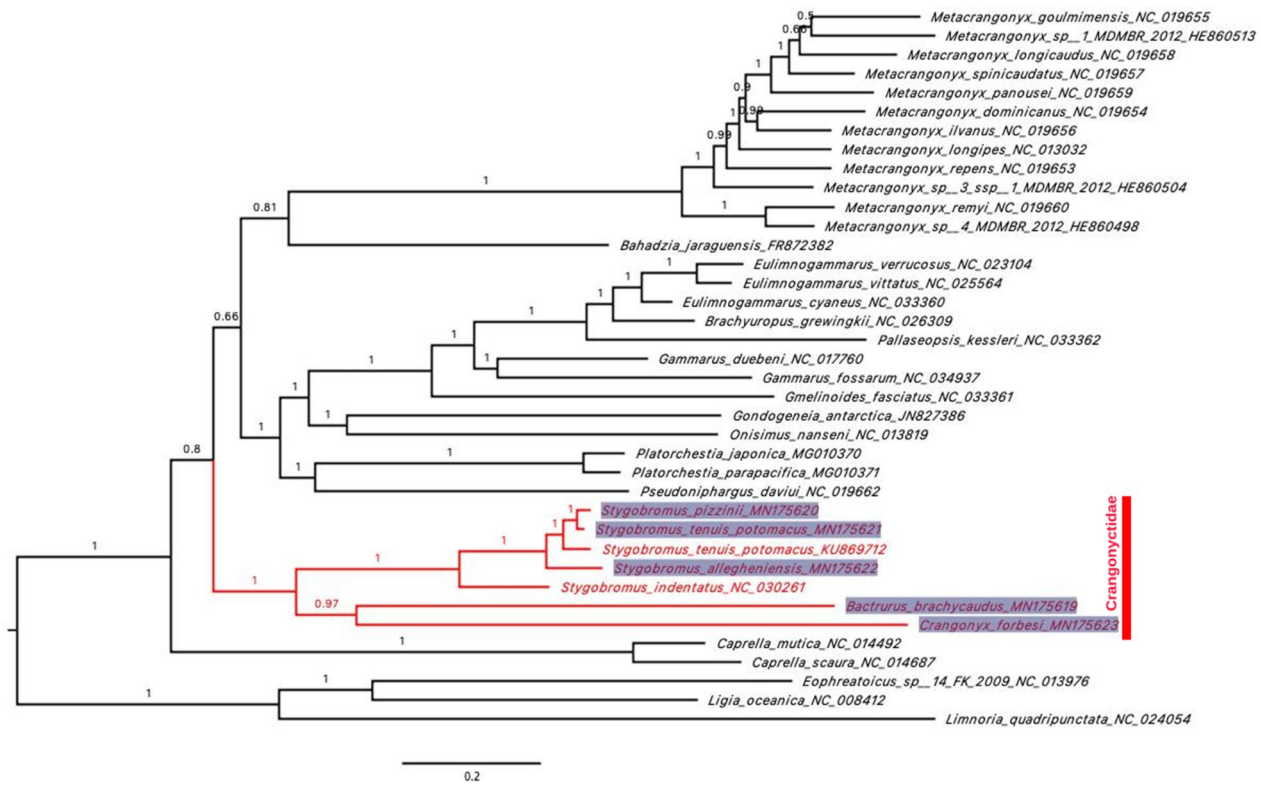

Fig. 4 Bayesian phylogeny of aligned protein-coding loci (3,607 amino acids) for five new amphipod mitogenomes (*Stygobromus allegheniensis, S. pizzinii, S. tenuis potomacus, Bactrurus brachycaudus,* and *Crangonyx forbesi*) in addition to 30 additional amphipod mitogenomes available on Genbank. The three isopods *Ligia oceanica, Limnoria quadripunctata,* and *Eophreatoicus sp.14 FK-2009* are included as an outgroup to root the phylogeny. New mitogenomes generated in this study are highlighted. GenBank accession numbers are included as suffix next to the species names. Values at nodes represent posterior probabilities

also exhibited a similar trend ($p=0.095$ and $p=0.057$, respectively) (Fig. 5). This could be because the rate at which slightly deleterious mutations (ω) responsible for the mitochondrial gene evolution accumulates comparatively faster in *cox* gene family of the surface lineages. However, this result is quite contradictory to previous studies showing higher functional constraint and conserved pattern in the genes coding for *cox* proteins than in other mitochondrial genes [119, 120].

To test if the 13 PCGs in subterranean lineages evolve at different relative rates compared to surface lineages, we compared a series of ML branch-based selection models (Table 3). For all PCG loci except *atp8*, *nad3*, and *nad4l* the saturated model (M2) where each branch had its own ω was favored. For *atp8*, *nad3*, and *nad4l* the best models were the M0 (single ω for all branches) and M1 (two ω model with one for surface and one for subterranean linages). In addition, the M1a model (six ω model with one for surface and one for each subterranean linage) was included in the set of best models for the *atp8* and *nad4l* loci. To further test if specific branches have undergone variable selective pressures, especially those amphipod branches adapted to surface habitats, we employed the two-ratio branch model. When the ω values for each PCG were compared between each amphipod terminal branch and the other 34 amphipod taxa, several loci in surface amphipod mitogenomes were found to be undergoing positive selection (ω1 > ω0; Fig. 6; Supplementary Table S8). This suggests that many surface amphipods have experienced directional selection in their mitochondrial loci perhaps due to high energy demands and was in accordance to previous studies in other arthropods [19, 32, 121, 122]. In contrast, several loci in subterranean amphipod mitogenomes have undergone purifying selection (ω1 < ω0). Surprisingly, a few loci in subterranean taxa displayed positive selection (ω1 > ω0; Fig. 6; Supplementary Table S8). To test if individual gene codons were subject to positive selection, we implemented two pairs of site models (M1a vs. M2a and M8a vs. M8). The M8 model identified one positively selected site on the *atp8* locus (37 N; $p=0$) and one positively selected site on the *nad5* locus (482 Q; $p=0$). Similarly, The M2a model identified two positively selected sites (37 N & 31 S; $p=0.0194$) on the *atp8* locus (Table 4).

Similar to flying grasshoppers that have evolved to adapt to increased energy demands to maintain the flight capacity [32], the mitochondrial loci of surface amphipods may have evolved mechanisms to meet increased energy demands due to predation, dispersal, and other factors. Although surface amphipods appear

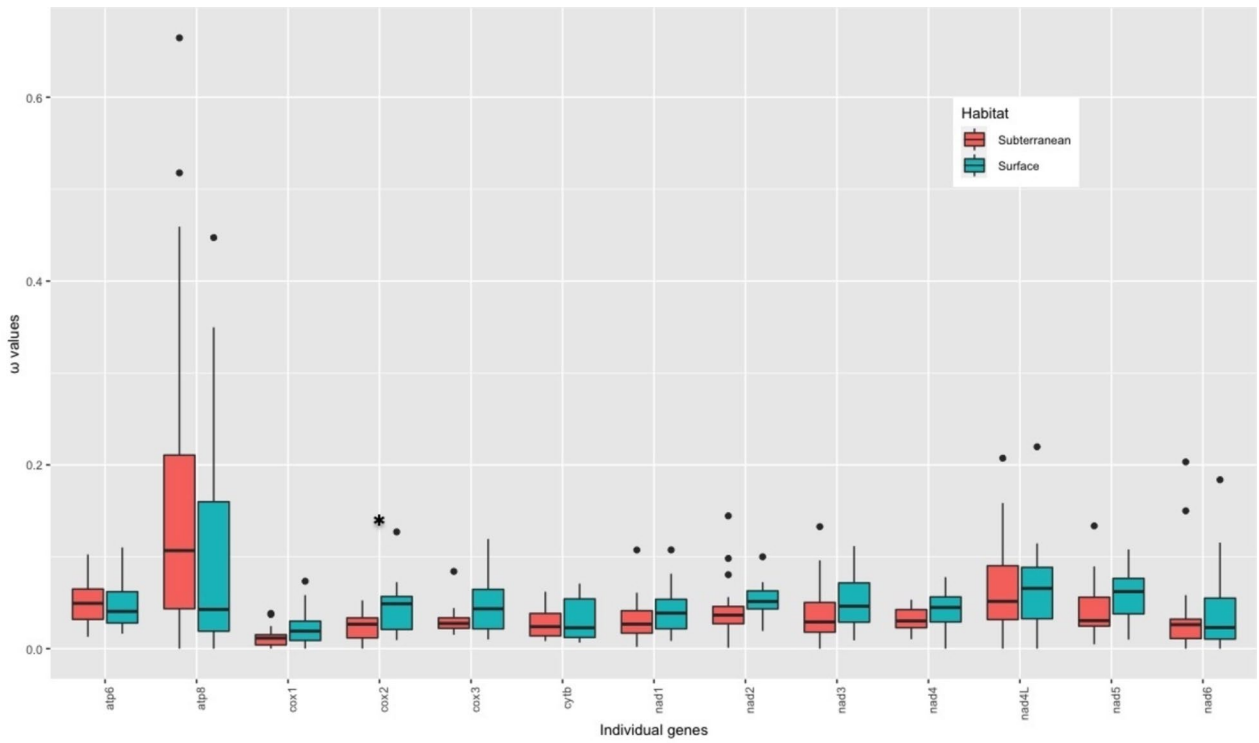

Fig. 5 Ratio of non-synonymous to synonymous substitutions (ω) in the 13 PCGs of subterranean (coral color) and surface (cyan color) amphipods based on the free-ratio model. Boxes include 50% of values; ω is not significantly different between subterranean and surface amphipods for any gene except *cox2** (*P* value = 0.02)

Table 3 AIC scores and ω estimates for various branch-based selection models for the 13 PCGs (one ω for all branches (M0), two-ratio model with background (surface) ω and single ω for subterranean branches (M1), two-ratio model with background (surface) ω and single ω for subterranean branches fixed at neutral evolution (ω = 1) (M1fixed), six-ratio model with background (surface) ω and a single ω for each subterranean lineage, B. brachycaudus (C1), Stygobromus clade (C2), B. jaraguensis (C3), Metacrangonyx clade (C4), P. daviui (C5) (M1a), and ω for each branch (M2)). The best-fit model(s) for each PCG is highlighted in red color

	Model M0		Model M1		Model M1fixed		Model M1a		Model M2	
Gene	AIC	ω estimates	AIC	ω estimates	AIC	ω estimates	AIC	ω estimates	AIC	ω estimates
atp6	30709.11	0.052	30705.55	Surface: 0.053, Subterranean: 0.051	32793.18	Surface: 0.036, Subterranean: 1.0	30720.21	Surface: 0.051, C1: 0.051, C2: 0.034, C3: 0.024, C4: 0.058, and C5: 0.207	30697.24	Surface: 0.016 - 0.222, Subterranean: 0.000 - 0.168
atp8	7990.16	0.130	7992.04	Surface: 0.157, Subterranean: 0.118	8113.73	Surface: 0.140, Subterranean: 1.0	7990.91	Surface: 0.160, C1: 0.122, C2: 0.186, C3: 0.081, C4: 0.084, and C5: 0.094	8056.30	Surface: 0.000 - 0.464, Subterranean: 0.000 - 0.295
cox1	49370.39	0.021	49369.70	Surface: 0.030, Subterranean: 0.015	57144.15	Surface: 0.019, Subterranean: 1.0	49267.64	Surface: 0.030, C1: 0.047, C2: 0.007, C3: 0.010, C4: 0.016, and C5: 0.039	48971.08	Surface: 0.000 - 0.401, Subterranean: 0.000 - 0.306
cox2	26060.41	0.030	26059.18	Surface: 0.046, Subterranean: 0.025	28836.01	Surface: 0.025, Subterranean: 1.0	26049.04	Surface: 0.047, C1: 0.005, C2: 0.019, C3: 0.007, C4: 0.028, and C5: 0.031	26035.93	Surface: 0.009 - 0.580, Subterranean: 0.000 - 0.098
cox3	32553.17	0.043	32553.32	Surface: 0.060, Subterranean: 0.033	35782.07	Surface: 0.040, Subterranean: 1.0	32509.67	Surface: 0.059, C1: 0.094, C2: 0.023, C3: 0.036, C4: 0.035, and C5: 0.037	32422.18	Surface: 0.010 - 0.310, Subterranean: 0.000 - 0.273
cytb	46946.99	0.033	46939.81	Surface: 0.037, Subterranean: 0.031	51249.18	Surface: 0.026, Subterranean: 1.0	46942.40	Surface: 0.037, C1: 0.047, C2: 0.026, C3: 0.041, C4: 0.032, and C5: 0.045	46766.62	Surface: 0.007 - 0.224, Subterranean: 0.007 - 0.839
nad1	38976.10	0.032	38976.74	Surface: 0.035, Subterranean: 0.031	42369.43	Surface: 0.028, Subterranean: 1.0	38999.49	Surface: 0.036, C1: 0.002, C2: 0.026, C3: 0.002, C4: 0.034, and C5: 0.198	38912.84	Surface: 0.008 - 0.112, Subterranean: 0.000 - 0.554
nad2	39812.50	0.044	39813.74	Surface: 0.059, Subterranean: 0.038	42292.24	Surface: 0.044, Subterranean: 1.0	39819.77	Surface: 0.059, C1: 0.087, C2: 0.028, C3: 0.018, C4: 0.042, and C5: 0.049	39787.04	Surface: 0.012 - 0.156, Subterranean: 0.000 - 0.119
nad3	14945.85	0.046	14947.23	Surface: 0.054, Subterranean: 0.041	15977.90	Surface: 0.040, Subterranean: 1.0	14949.81	Surface: 0.055, C1: 0.065, C2: 0.037, C3: 0.027, C4: 0.043, and C5: 0.063	14969.42	Surface: 0.000 - 0.112, Subterranean: 0.000 - 0.135
nad4	59119.83	0.043	59121.56	Surface: 0.059, Subterranean: 0.037	63490.21	Surface: 0.043, Subterranean: 1.0	59083.83	Surface: 0.059, C1: 0.030, C2: 0.034, C3: 0.003, C4: 0.038, and C5: 0.039	58905.61	Surface: 0.011 - 0.159, Subterranean: 0.002 - 0.145
nad4l	13872.06	0.038	13872.35	Surface: 0.059, Subterranean: 0.032	14644.27	Surface: 0.042, Subterranean: 1.0	13870.75	Surface: 0.065, C1: 0.011, C2: 0.024, C3: 0.056, C4: 0.034, and C5: 0.176	13887.45	Surface: 0.000 - 0.226, Subterranean: 0.000 - 0.226
nad5	85434.08	0.061	85435.64	Surface: 0.074, Subterranean: 0.054	90271.17	Surface: 0.056, Subterranean: 1.0	85455.26	Surface: 0.075, C1: 0.083, C2: 0.054, C3: 0.025, C4: 0.055, and C5: 0.063	85032.23	Surface: 0.010 - 0.109, Subterranean: 0.013 - 0.132
nad6	22465.81	0.044	22467.35	Surface: 0.056, Subterranean: 0.037	23588.74	Surface: 0.037, Subterranean: 1.0	22456.51	Surface: 0.054, C1: 0.047, C2: 0.033, C3: 0.004, C4: 0.040, and C5: 0.042	22428.97	Surface: 0.000 - 0.180, Subterranean: 0.000 - 0.138

to be evolving under selective pressures different from those of the subterranean taxa and their mitochondrial loci have accumulated more nonsynonymous than synonymous mutations compared to subterranean taxa, the branch model tests did not clearly support positive selection on these branches, and we cannot rule out the influence of relaxed selection. Previous studies have demonstrated that positive selection will act on only a few sites for a short period of evolutionary time, and a signal of positive selection often is overwhelmed by continuous negative selection that sweeps across most sites in a gene sequence [123].

In contrast to branch models where ω varies only among branches, branch-site models allow selection to vary both among amino acid sites and lineages. Thus, branch-site models are considered quite useful in distinguishing positive selection from relaxed or purifying selection [123]. Using the more stringent branch-site model, we detected positive selection in 14 branches and 12 loci with a total of 308 amino acid sites under

Table 4 Evidence of positive selection on the mitochondrial PCGs of subterranean and surface-dwelling amphipods based on site model

Model	np	Ln L	Estimates of parameters				Model compared	LRT *P*-value	Positive sites	Gene
M2a	72	-4021.125381	p:	0.32097	0.56570	0.11334	M1a vs. M2a	0.019437929	31 S 0.977*, 37 N 0.997**	*atp8*
			ω:	0.09324	1.00000	2.44333				
M1a	70	-4025.065910	p:	0.37651	0.62349					
			ω:	0.09961	1.00000					
M8	72	-3950.635672	p0 = 0.85323	*p* = 0.54776	q = 3.55619		M8a vs.M8	0.000013424	37 N 0.875	
			(p1 = 0.14677)	ω = 1.00000						
M8a	71	-3941.161040	p0 = 0.97880	*p* = 0.73512	q = 3.74996					
			(p1 = 0.02120)	ω = 1.00000						
M2a	72	-42238.654620	p:	0.85660	0.08524	0.05815	M1a vs. M2a	1.000000000	482 Q 0.524	*nad5*
			ω:	0.07211	1.00000	1.00000				
M1a	70	-42238.654620	p:	0.85660	0.14340					
			ω:	0.07211	1.00000					
M8	72	-40545.492521	p0 = 0.98460	*p* = 0.53211	q = 7.22545		M8a vs.M8	0.000000000	482 Q 0.856	
			(p1 = 0.01540)	ω = 1.00000						
M8a	71	-40454.428911	p0 = 0.99711	*p* = 0.50047	q = 6.79227					
			(p1 = 0.00289)	ω = 1.00000						

* highlights a statistically significant (LRT *P*-value < 0.05) positively selected site (BEB: $P \geq 95\%$)

** highlights a statistically significant (LRT *P*-value < 0.05) positively selected site (BEB: $P \geq 99\%$)

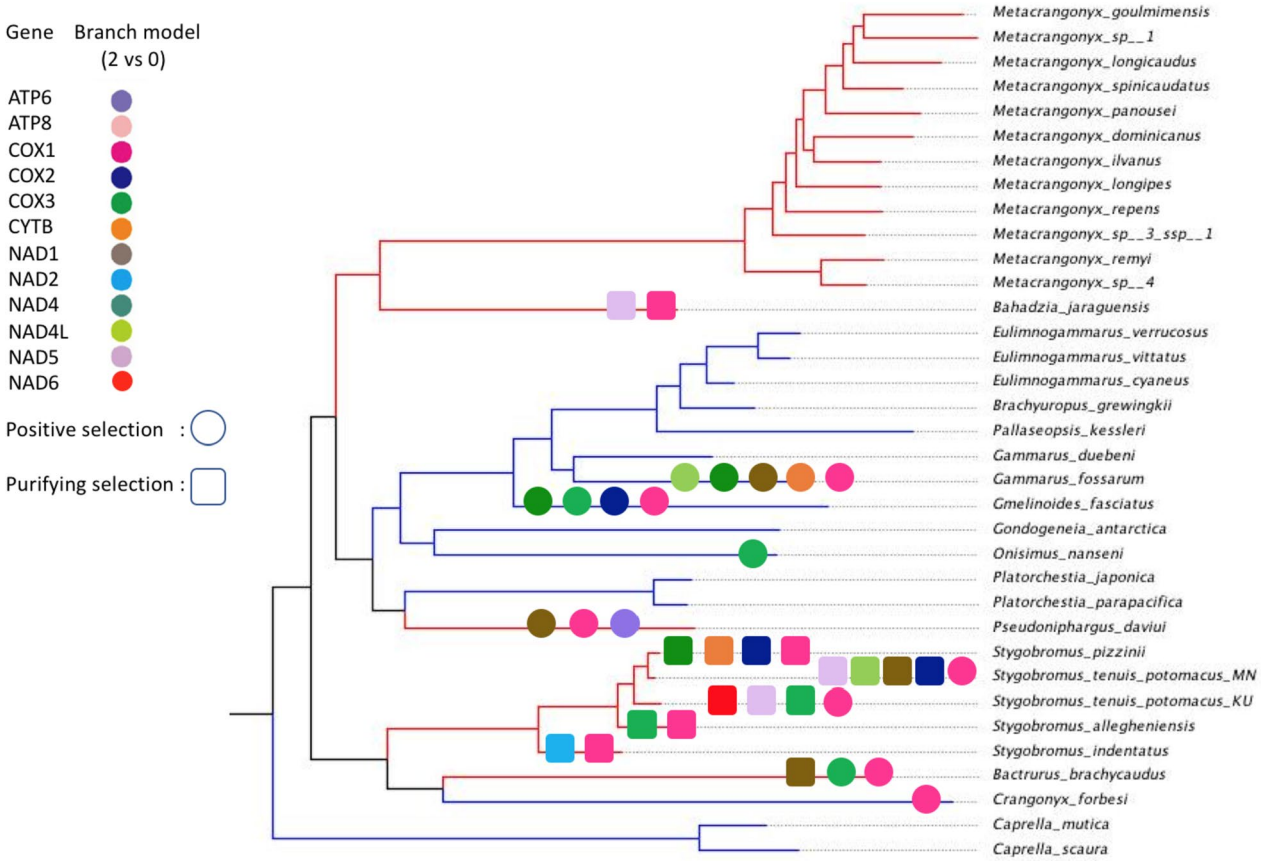

Fig. 6 Results of selective pressure analysis of mitochondrial PCGs with LRT *P*-value < 0.05 in subterranean and surface-dwelling lineages of amphipods based on branch 2 vs. 0 model. Different colored shapes represent different mitochondrial genes. Squares represent purifying selection and circles represent positive selection. Surface amphipod branches are colored blue and subterranean amphipod branches are colored red

positive selection. Among them, 80 amino acid sites in seven loci (*atp6*, *atp8*, *cox3*, *nad2*, *nad3*, *nad4*, and *nad5*) were identified on the subterranean terminal branches, whereas 228 amino acid sites in 10 loci (*atp6*, *atp8*, *cox1*, *cox2*, *cytb*, *nad1*, *nad2*, *nad3*, *nad5*, and *nad6*) were identified on the surface terminal branches. Nearly three times as many positively selected amino acid sites were detected on surface branches compared to subterranean branches. Most of the positively selected loci on surface branches were found in *C. forbesi* with 114 sites (Fig. 7; Supplementary Table S9). In total, eight positive selected loci (*atp6*, *atp8*, *cox1*, *cox2*, *cytb*, *nad1*, *nad4*, and *nad5*) were identified by the branch-site model and by at least one other model on the surface branches, whereas only four positive selected genes (*atp6*, *atp8*, *cox3*, and *nad5*) were identified on the subterranean branches.

The identification of many positively selected amino acid sites suggests that episodic positive selection has acted on mitochondrial PCGs of surface amphipods. In addition, we also identified a few positively selected sites on subterranean branches primarily in *B. brachycaudus* with 39 sites and *P. daviui* with 25 sites (Supplementary Table S9). *Bactrurus brachycaudus* is usually associated with springs and caves [124], while *P. daviui* is associated with groundwater wells [77].

Direction and magnitude of selection pressures

Given the crucial role played by the mitochondrial genome in metabolic energy production [125], we hypothesized that the mitogenome of surface amphipods may show evidence of adaptation (directional selection) to life in surface habitats where energy demand is higher relative to subterranean habitats. We found support for directional selection in surface lineages based on three different selection analyses (RELAX, aBSREL, and BUSTED). In summary, all tests confirmed the existence of a moderate signal of positive or diversifying selection, as well as signal for significant relaxed purifying

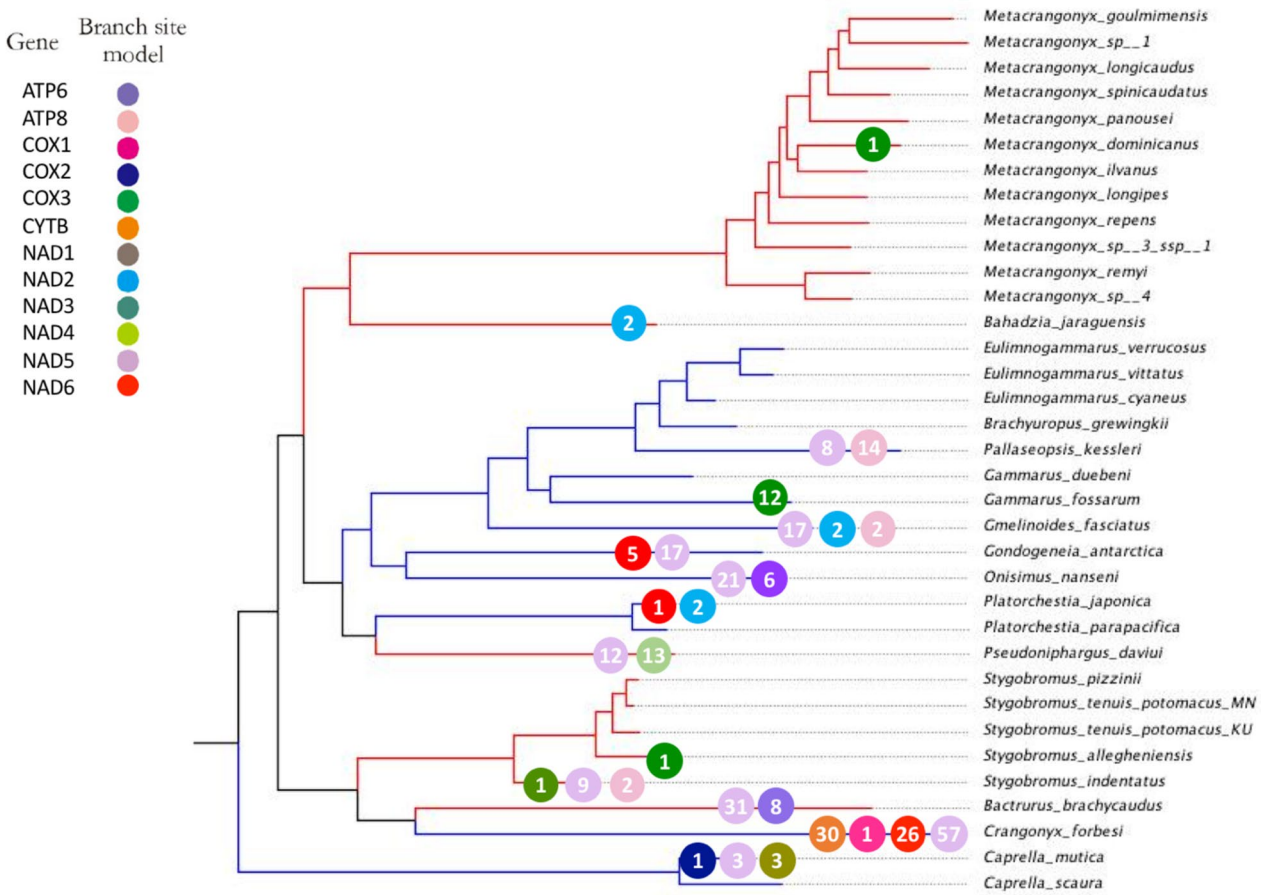

Fig. 7 Evidence of positive selection on the mitochondrial PCGs (LRT $P<0.05$) and positively selected site (BEB: $P\geq95\%$) in subterranean and surface-dwelling lineages of amphipods based on branch-site models. Different colored circles represent different mitochondrial loci. The number within each circle represents the number of positive selection sites detected for the locus. Surface amphipod branches are colored blue and subterranean amphipod branches are colored red

selection in the mitogenome of surface amphipods. This supports a previous study by Carlini and Fong [126] who reported evidence for relaxation of functional evolutionary constraints (positive or diversifying selection) in the transcriptome of a subterranean amphipod *Gammarus minus*.

We implemented aBSREL on the concatenated 13 PCG dataset comprising all 35 species as test branches and detected episodic diversifying selection in seven species: *P. daviui* ($p=0$), *O. nanseni* ($p=0.0008$), *G. fasciatus* ($p=0.0298$), *G. fossarum* ($p=0.045$), *B. jaraguensis* ($p=0.0016$), *C. forbesi* ($p=0$), and *B. brachycaudus* ($p=0.0001$). We then used aBSREL to conduct independent tests for the crangonyctid species as the test branch and the remaining species as reference branches. We detected evidence of episodic diversifying selection in *C. forbesi* ($p=0$) and *B. brachycaudus* ($p=0.0001$) (Table 5). Using BUSTED, which provides a gene-wide test for positive selection, we detected evidence of episodic diversifying selection in three of the surface species: *C. forbesi* ($p=0.011$), *G. fasciatus* ($p=0.033$), *G. antarctica* ($p=0.009$), whereas evidence of gene-wide episodic diversifying selection was found in just one of the subterranean species, *P. daviui* ($p=0.020$) (Table 5). Using RELAX, which tests whether the strength of selection has been relaxed or intensified along a specified set of test branches, we detected selection evidence of relaxed selection in *C. forbesi* ($p=0$) and other surface species, including *O. nanseni, G. fasciatus, G. fossarum, G. antarctica*, and *P. kessleri*. Contrastingly, evidence of intensification of selection was detected in subterranean species, including *S. tenuis* ($p=0$), *S. allegheniensis* ($p=0.0025$), *S. indentatus* ($p=0$), and *S. pizzinii* ($p=0$). Surprisingly, a few of the surface species including *C. mutica* ($p=0.015$), *E. cyaneus* ($p=0$), and *P. japonica* ($p=0$) exhibited intensification of selection and subterranean species including *P. daviui* ($p=0$) and *M. dominicanus* ($p=0.015$) exhibited relaxation of selection (Table 5).

In addition to the concatenated 13 PCG dataset, we also conducted selection analyses for each PCG to determine which genes might be evolving under unique selection pressures. We found evidence of directional selection in *atp8* of *C. forbesi* ($p=0.026$) and *nad3* of *S. pizzinii* ($p=0.041$) using aBSREL and *cox3* of *B. brachycaudus*

Table 5 Selection signals in the mitogenomes of amphipods inferred using aBSREL, BUSTED, and RELAX algorithms. The dataset comprising all 13 concatenated protein-coding genes with 3,607 amino acid sites in the alignment. K column: a statistically significant $K>1$ indicates that selection strength has been intensified, and $K<1$ indicates that selection strength has been relaxed. LR is likelihood ratio and D indicates the direction of selection pressure change: intensified (I) or relaxed (R), where * highlights a statistically significant ($p<0.05$) result. Mitogenomes with significant LRT *P* -value < 0.05 are highlighted in red color

		aBSREL	BUSTED		RELAX		
Species	Genes-Sites	p-value	p-value	K	p-value	LR	D
Crangonyx forbesi	13PCG-3607	0.000	0.011	0.00	0.000	146.46	R*
Gmelinoides fasciatus	13PCG-3607	0.030	0.033	0.24	0.000	174.12	R*
Onisimus nanseni	13PCG-3607	0.001	0.500	0.25	0.000	80.59	R*
Gammarus fossarum	13PCG-3607	0.045	0.500	0.43	0.000	94.94	R*
Caprella mutica	13PCG-3607	0.500	0.500	1.12	0.015	5.97	I*
Eulimnogammarus cyaneus	13PCG-3607	0.500	0.448	2.20	0.000	77.75	I*
Platorchestia japonica	13PCG-3607	0.500	0.500	1.90	0.000	57.20	I*
Gondogeneia antarctica	13PCG-3607	0.500	0.009	0.28	0.000	49.83	R*
Pallaseopsis kessleri	13PCG-3607	0.500	0.500	1.00	0.000	15.68	R*
Brachyuropus grewingkii	13PCG-3607	0.500	0.500	1.03	0.624	0.24	I
Pseudoniphargus daviui	13PCG-3607	0.000	0.020	0.63	0.000	2721.06	R*
Metacrangonyx dominicanus	13PCG-3607	0.500	0.293	0.88	0.015	5.89	R*
Bahadzia jaraguensis	13PCG-3607	0.002	0.500	0.90	0.116	2.47	R
Bactrurus brachycaudus	13PCG-3607	0.000	0.500	0.90	0.119	2.43	R
Stygobromus tenuis potomacus_MN	13PCG-3607	0.500	0.500	48.44	0.000	66.82	I*
Stygobromus tenuis potomacus_KU	13PCG-3607	0.500	0.500	1.17	0.739	0.11	I
Stygobromus allegheniensis	13PCG-3607	0.500	0.500	49.37	0.025	5.02	I*
Stygobromus pizzinii	13PCG-3607	0.500	0.500	1.27	0.000	1852.16	I*
Stygobromus indentatus	13PCG-3607	0.500	0.500	1.28	0.000	16.42	I*

($p = 0.029$) using BUSTED. *Atp8* of the surface amphipod *C. forbesi* exhibited strong evidence of directional selection, which was quite surprising as *atp8* is a small locus sometimes missing from metazoan mitogenomes and normally evolves under highly relaxed selection pressures [127]. RELAX analyses uncovered five loci (*cox1*, *cox3*, *cytb*, *nad1*, and *nad3*) that exhibited relaxed selection and one gene (*atp6*) that exhibited intensification of selection in *C. forbesi*. Similarly, three loci (*cox3, nad5*, and *nad6*) in *B. brachycaudus* showed evidence of relaxed selection. Several loci in other subterranean species, including S. *tenuis, S. allegheniensis*, and *S. pizzinii*, exhibited varying levels of intensification of selection, whereas none exhibited relaxed selection (Table 6). Some of these outliers were expected, as *nad5* and *nad6* are known to evolve faster among the mitochondrial loci [128]. Also, evidence for relaxation of functional evolutionary constraints (positive or diversifying selection) has been reported in the *nad* family of subterranean *Gammarus* species adapted to the subterranean environment [126]. Although this may explain outliers in the subterranean *B. brachycaudus* mitogenome, it remains unclear why *cox3* exhibited signatures of relaxed selection. This gene is generally one of the most conserved mitochondrial loci in animals [92, 129, 130], and high levels of purifying selection has been observed in the *cox* family in other amphipod species [29]. In *C. forbesi*, *atp6* showed signatures of positive selection, which contrasted most other PCGs in its mitogenome that exhibited relaxed selection. Overall, in accordance with the results obtained using the concatenated dataset, individual mitochondrial loci of subterranean amphipods mostly exhibited varying levels of purifying selection, whereas surface amphipods predominantly exhibited more relaxed selection.

To provide further evidence of positive selection, we implemented the RELAX, aBSREL, and BUSTED algorithms on the branch, branch-site, and site models. Eight loci (*atp8*, *cox1*, *cox2*, *cytb*, *nad1*, *nad4*, *nad5*, and *nad6*) all involved in the OXPHOS pathway were under positive selection in surface branches by at least two methods. The loci *nad1*, *nad4*, *nad5*, and *nad6* encode the subunits of NADH dehydrogenase, also called Complex I, that initiates the oxidative phosphorylation process. Complex I is the largest and most complicated proton pump of the respiratory chain and is involved in electron transfer from NADH to ubiquinone to supply the proton motive force used for ATP synthesis [131], Complex I plays a key role in cellular energy metabolism by pumping gradient of protons across the mitochondrial membrane producing more than one-third of mitochondrial energy [132]. Genes *cox1* & *cox2* encode the catalytic core of Cytochrome c oxidase also called Complex IV. Complex IV is directly involved in electron transfer and proton translocation [133]. Gene *atp8* encodes a part of ATP synthase, also called Complex V, and plays a major role in the final assembly of ATPase [133]. In summary, our selection analyses revealed signals of positive selection in several mitochondrial genes of surface amphipods, which

Table 6 Selection signals in the mitochondrial PCGs of crangonyctid amphipods sequenced in this study inferred using aBSREL, BUSTED, and RELAX algorithms. K column: a statistically significant $K > 1$ indicates that selection strength has been intensified, and $K < 1$ indicates that selection strength has been relaxed. LR is likelihood ratio and D indicates the direction of selection pressure change: intensified (I) or relaxed (R), where * highlights a statistically significant ($p < 0.05$) result. PCGs with significant LRT *P* -value < 0.05 are highlighted in red color

		Crangonyx forbesi				*Bactrurus brachycaudus*				*Stygobromus tenuis potomacus*				*Stygobromus allegheniensis*				*Stygobromus pizzinii*			
		aBSREL	BUSTED	RELAX		aBSREL	BUSTED	RELAX		aBSREL	BUSTED	RELAX		aBSREL	BUSTED	RELAX		aBSREL	BUSTED	RELAX	
Gene	Sites	p-value	p-value	p-value	D	p-value	p-value	p-value	D	p-value	p-value	p-value	D	p-value	p-value	p-value	D	p-value	p-value	p-value	D
atp6	218	0.500	0.272	0.001	I*	0.500	0.357	0.648	R	1.000	0.500	1.000	R	0.069	0.500	0.000	I*	1.000	0.500	0.127	I
atp8	50	0.026	0.229	0.625	I	1.000	0.500	0.214	I	0.500	0.500	0.510	R	0.435	0.478	0.142	R	0.444	0.500	0.336	R
cox1	511	0.056	0.146	0.000	R*	0.105	0.500	1.000	R	1.000	0.500	0.000	I*	1.000	0.500	0.150	I	1.000	0.500	0.044	I*
cox2	222	0.500	0.476	0.634	I	0.188	0.280	0.262	R	1.000	0.500	0.017	I*	0.500	0.500	0.359	I	1.000	0.500	0.096	I
cox3	262	1.000	0.500	0.032	R*	0.199	0.029	0.023	R*	1.000	0.500	1.000	R	1.000	0.500	0.000	I*	0.367	0.500	0.018	I*
cytb	377	0.143	0.500	0.000	R*	0.500	0.500	0.112	I	1.000	0.500	0.080	I	0.230	0.500	0.672	I	1.000	0.500	0.536	I
nad1	305	0.093	0.500	0.000	R*	1.000	0.500	0.067	I	1.000	0.500	0.001	I*	0.151	0.500	0.034	I*	1.000	0.500	0.125	I
nad2	321	1.000	0.500	0.386	R	1.000	0.500	0.363	R	1.000	0.500	0.220	I	1.000	0.500	0.002	I*	1.000	0.500	0.141	I
nad3	116	0.414	0.308	0.000	R*	1.000	0.500	0.752	R	1.000	0.500	0.000	I*	0.500	0.500	0.118	I	0.041	0.500	0.149	R
nad4	435	1.000	0.146	0.068	R	1.000	0.500	0.482	I	1.000	0.500	0.076	I	1.000	0.500	0.105	I	1.000	0.500	0.008	I*
nad4l	94	1.000	0.500	0.978	I	1.000	0.500	0.854	I	1.000	0.500	0.018	I*	0.500	0.500	0.980	I	1.000	0.500	1.000	I
nad5	552	1.000	0.500	0.774	I	0.088	0.479	0.024	R*	1.000	0.500	0.005	I*	0.447	0.500	0.012	I*	1.000	0.500	0.003	I*
nad6	144	0.500	0.500	0.250	R	1.000	0.500	0.036	R*	1.000	0.500	0.643	R	1.000	0.500	0.517	I	0.500	0.500	0.680	R

may be associated with increased energy demands in surface environments. In contrast, subterranean amphipods showed signatures of purifying selection, which may be related to maintaining efficient energy metabolism in subterranean habitats.

Conclusion

In this study, we compared mitogenome features including AT/GC-skew, codon usage, gene order, phylogenetic relationships, and selection pressures acting upon amphipods inhabiting surface and subterranean habitats. We described a novel mitochondrial gene order for *C. forbesi*. We identified a signal of directional selection in the protein-encoding genes of the OXPHOS pathway in the mitogenomes of surface amphipods and a signal of purifying selection in subterranean species, which is consistent with the hypothesis that the mitogenome of surface-adapted amphipods has evolved in response to a more energy demanding environment compared to subterranean species. Our comparative analyses of gene order, locations of non-coding regions, and base-substitution rates points to habitat as an important factor influencing the evolution of amphipod mitogenomes. However, the generation and study of mitogenomes from additional amphipod taxa, including other crangonyctid species, are needed to better elucidate phylogenetic relationships and the evolution of mitogenomes of amphipods, as mitogenomes are available for just a tiny fraction of the more than 10,000 described amphipods. In addition, more evidence is needed to further validate our inferences, such as studying the effects of amino acid changes on three-dimensional protein structure and function. Nevertheless, our study provides a necessary foundation for the study of mitogenome evolution in amphipods and other crustaceans.

Supplementary Information

The online version contains supplementary material available at https://doi.org/10.1186/s12864-024-10111-w.

Supplementary Material 1.

Acknowledgements

The authors would like to thank David C. Culver, Daniel W. Fong, Steven J. Taylor, and Kayla Wilson for collecting specimens. We also thank David Young from Alabama Supercomputer Center for providing assistance with troubleshooting and program installation on the high-performance computing cluster.

Authors' contributions

Authors Joseph B. Benito and Matthew L. Niemiller contributed to conceptualization, data collection and curation, and manuscript writing and reviewing. Author Megan L. Porter contributed to manuscript writing and reviewing.

Funding

This study was supported by a grant from the Friends of the Capital Crescent Trail, the town of Chevy Chase, Illinois Natural History Survey, and The University of Alabama in Huntsville.

Availability of data and materials

The data that support the findings of this study are openly available in NCBI GenBank at https://www.ncbi.nlm.nih.gov/nuccore/MN175619.1 (Bactrurus brachycaudus), https://www.ncbi.nlm.nih.gov/nuccore/MN175620.1 (Stygobromus pizzinii), https://www.ncbi.nlm.nih.gov/nuccore/MN175621.1 (Stygobromus tenuis potomacus), https://www.ncbi.nlm.nih.gov/nuccore/MN175622.1 (Stygobromus allegheniensis), and https://www.ncbi.nlm.nih.gov/nuccore/MN175623.1 (Crangonyx forbesi).
The sample voucher numbers, related meta-data, and raw sequencing data are openly available in NCBI SRA RunSelector at https://www.ncbi.nlm.nih.gov/Traces/study/?acc=PRJNA657640.

Declarations

Ethics approval and consent to participate

Not applicable.

Consent for publication

Not applicable.

Competing interests

The authors declare no competing interests.

Author details

[1]Department of Biological Sciences, The University of Alabama in Huntsville, Huntsville, AL 35899, USA. [2]School of Life Sciences, University of Hawai'i at Mānoa, Honolulu, HI 96822, USA.

Received: 20 June 2023 Accepted: 9 February 2024
Published online: 20 March 2024

References

1. Culver DC, Pipan T. The biology of caves and other subterranean habitats. Oxford: Oxford University Press; 2009.
2. Soares D, Niemiller ML. Extreme adaptation in caves. Anat Rec. 2020;303(1):15–23.
3. Dröse S, Krack S, Sokolova L, Zwicker K, Barth HD, Morgner N, Brandt U. Functional dissection of the proton pumping modules of mitochondrial complex I. PLoS Biol. 2011;9(8):e1001128.
4. Pons J, Bauzà-Ribot MM, Jaume D, Juan C. Next-generation sequencing, phylogenetic signal and comparative mitogenomic analyses in Metacrangonyctidae (Amphipoda: Crustacea). BMC Genomics. 2014;15(1):1–16.
5. Porter ML, Engel AS, Kane TC, Kinkle BK. Productivity-diversity relationships from chemolithoautotrophically based sulfidic karst systems. Int J Speleol. 2009;38(1):4.
6. Simon KS, Benfield EF. Leaf and wood breakdown in cave streams. J North Am Benthological Soc. 2001;20(4):550–63.
7. Gissi C, Iannelli F, Pesole G. Evolution of the mitochondrial genome of Metazoa as exemplified by comparison of congeneric species. Heredity. 2008;101(4):301–20.
8. Horton T, Thurston MH, Vlierboom R, Gutteridge Z, Pebody CA, Gates AR, Bett BJ. Are abyssal scavenging amphipod assemblages linked to climate cycles? Prog Oceanogr. 2020;184:102318.
9. Huntsman BM, Venarsky MP, Benstead JP, Huryn AD. Effects of organic matter availability on the life history and production of a top vertebrate predator (Plethodontidae: *Gyrinophilus palleucus*) in two cave streams. Freshw Biol. 2011;56(9):1746–60.
10. Venarsky MP, Huntsman BM, Huryn AD, Benstead JP, Kuhajda BR. Quantitative food web analysis supports the energy-limitation hypothesis in cave stream ecosystems. Oecologia. 2014;176(3):859–69.
11. Crozier RH, Crozier YC. The mitochondrial genome of the honeybee *Apis mellifera*: complete sequence and genome organization. Genetics. 1993;133(1):97–117.
12. Ito A, Aoki MN, Yokobori SI, Wada H. The complete mitochondrial genome of *Caprella scaura* (Crustacea, Amphipoda, Caprellidea), with emphasis on the unique gene order pattern and duplicated control region. Mitochondrial DNA. 2010;21(5):183–90.

13. Hassanin A, Ropiquet A, Couloux A, Cruaud C. Evolution of the mitochondrial genome in mammals living at high altitude: new insights from a study of the tribe Caprini (Bovidae, Antilopinae). J Mol Evol. 2009;68(4):293–310.
14. Hyde J, Cooper SJ, Munguia P, Humphreys WF, Austin AD. The first complete mitochondrial genomes of subterranean dytiscid diving beetles (*Limbodessus* and *Paroster*) from calcrete aquifers of Western Australia. Aust J Zool. 2018;65(5):283–91.
15. Bishop R, Humphreys WF, Longley G. Epigean and Hypogean *Palaemonetes* sp. (Decapoda, Palaemonidae) from Edwards Aquifer: an examination of trophic structure and metabolism. Subterr Biol. 2014;14:79–102.
16. Murrell B, Weaver S, Smith MD, Wertheim JO, Murrell S, Aylward A, Kosakovsky Pond SL. Gene-wide identification of episodic selection. Mol Biol Evol. 2015;32(5):1365–71.
17. Da Fonseca RR, Johnson WE, O'Brien SJ, Ramos MJ, Antunes A. The adaptive evolution of the mammalian mitochondrial genome. BMC Genomics. 2008;9(1):1–22.
18. Shen YY, Shi P, Sun YB, Zhang YP. Relaxation of selective constraints on avian mitochondrial DNA following the degeneration of flight ability. Genome Res. 2009;19(10):1760–5.
19. Yang Y, Xu S, Xu J, Guo Y, Yang G. Adaptive evolution of mitochondrial energy metabolism genes associated with increased energy demand in flying insects. PLoS One. 2014;9(6):e99120.
20. Boore JL. Animal mitochondrial genomes. Nucleic Acids Res. 1999;27(8):1767–80.
21. Burger G, Gray MW, Lang BF. Mitochondrial genomes: anything goes. Trends Genet. 2003;19(12):709–16.
22. Xu S, Luosang J, Hua S, He J, Ciren A, Wang W, Zheng X. High altitude adaptation and phylogenetic analysis of tibetan horse based on the mitochondrial genome. J Genet Genomics. 2007;34(8):720–9.
23. Ballard JWO, Pichaud N. Mitochondrial DNA: more than an evolutionary bystander. Funct Ecol. 2014;28(1):218–31.
24. Bourguignon T, Tang Q, Ho SY, Juna F, Wang Z, Arab DA, Lo N. Transoceanic dispersal and plate tectonics shaped global cockroach distributions: evidence from mitochondrial phylogenomics. Mol Biol Evol. 2018;35(4):970–83.
25. Zou H, Jakovlić I, Zhang D, Chen R, Mahboob S, Al-Ghanim KA, Wang GT. The complete mitochondrial genome of *Cymothoa indica* has a highly rearranged gene order and clusters at the very base of the Isopoda clade. PLoS One. 2018;13(9):e0203089.
26. Culver DC, Kane TC, Fong DW. Adaptation and natural selection in caves: the evolution of *Gammarus minus*. Cambridge: Harvard University Press; 1995. p. 223.
27. Shen YY, Liang L, Zhu ZH, Zhou WP, Irwin DM, Zhang YP. Adaptive evolution of energy metabolism genes and the origin of flight in bats. Proc Natl Acad Sci. 2010;107(19):8666–71.
28. Botero-Castro F, Tilak MK, Justy F, Catzeflis F, Delsuc F, Douzery EJ. In cold blood: compositional bias and positive selection drive the high evolutionary rate of vampire bats mitochondrial genomes. Genome Biol Evol. 2018;10(9):2218–39.
29. Sun S, Wu Y, Ge X, Jakovlić I, Zhu J, Mahboob S, Fu H. Disentangling the interplay of positive and negative selection forces that shaped mitochondrial genomes of *Gammarus pisinnus* and*Gammarus lacustris*. Royal Soc Open Sci. 2020;7(1):190669.
30. Gao F, Chen C, Arab DA, Du Z, He Y, Ho SY. EasyCodeML: a visual tool for analysis of selection using CodeML. Ecol Evol. 2019;9(7):3891–8.
31. Welch AJ, Bedoya-Reina OC, Carretero-Paulet L, Miller W, Rode KD, Lindqvist C. Polar bears exhibit genome-wide signatures of bioenergetic adaptation to life in the arctic environment. Genome Biol Evol. 2014;6(2):433–50.
32. Li M, Jin L, Ma J, Tian S, Li R, Li X. Detecting mitochondrial signatures of selection in wild tibetan pigs and domesticated pigs. Mitochondrial DNA Part A. 2016;27(1):747–52.
33. Mitterboeck TF, Liu S, Adamowicz SJ, Fu J, Zhang R, Song W, Zhou X. Positive and relaxed selection associated with flight evolution and loss in insect transcriptomes. GigaScience. 2017;6(10):gix073.
34. Beall CM. Two routes to functional adaptation: Tibetan and Andean high-altitude natives. Proc Natl Acad Sci. 2007;104(suppl 1):8655–60.
35. Scott GR, Schulte PM, Egginton S, Scott AL, Richards JG, Milsom WK. Molecular evolution of cytochrome c oxidase underlies high-altitude adaptation in the bar-headed goose. Mol Biol Evol. 2011;28(1):351–63.
36. Oliveira DC, Raychoudhury R, Lavrov DV, Werren JH. Rapidly evolving mitochondrial genome and directional selection in mitochondrial genes in the parasitic wasp *Nasonia* (Hymenoptera: Pteromalidae). Mol Biol Evol. 2008;25(10):2167–80.
37. Yang Z. PAML 4: phylogenetic analysis by maximum likelihood. Mol Biol Evol. 2007;24(8):1586–91.
38. Letunic I, Bork P. Interactive tree of life (iTOL) v5: an online tool for phylogenetic tree display and annotation. Nucleic Acids Res. 2021;49(W1):W293–6.
39. Arfianti T, Wilson S, Costello MJ. Progress in the discovery of amphipod crustaceans. PeerJ. 2018;6:e5187.
40. Hervant F, Mathieu J, Barré H, Simon K, Pinon C. Comparative study on the behavioral, ventilatory, and respiratory responses of hypogean and epigean crustaceans to long-term starvation and subsequent feeding. Comp Biochem Physiol A. 1997;118(4):1277–83.
41. Barnard JL, Karaman GS. The families and genera of marine gammaridean Amphipoda (except marine gammaroids). Records Aust Museum Suppl. 1991;13(1/2):1–866.
42. Bousfield EL. An updated phyletic classification and palaeohistory of the Amphipoda. Crustacean Issues. 1983;1:257–77.
43. Huppop K. How do cave animals cope with the food scarcity in caves? In: Wilkens H, Culver DC, Humphreys WF, editors. Ecosystems of the world. Subterranean ecosystems. Vol. 30. Amsterdam: Elsevier; 2000. p. 159–188.
44. Dotson EM, Beard C. Sequence and organization of the mitochondrial genome of the Chagas disease vector, *Triatoma dimidiata*. Insect Mol Biol. 2001;10(3):205–15.
45. Wu X, Wang L, Chen S, Zan R, Xiao H, Zhang YP. The complete mitochondrial genomes of two species from *Sinocyclocheilus* (Cypriniformes: Cyprinidae) and a phylogenetic analysis within Cypininae. Mol Biol Rep. 2010;37(5):2163–71.
46. Graening GO, Brown AV. Ecosystem dynamics and pollution effects in an Ozark cave stream 1. JAWRA J Am Water Resour Assoc. 2003;39(6):1497–507.
47. Poulson TL, White WB. The Cave Environment: limestone caves provide unique natural laboratories for studying biological and geological processes. Science. 1969;165(3897):971–81.
48. Protas ME, Trontelj P, Patel NH. Genetic basis of eye and pigment loss in the cave crustacean, *Asellus aquaticus*. Proc Natl Acad Scie. 2011;108(14):5702–7.
49. Qiu Q, Zhang G, Ma T, Qian W, Wang J, Ye Z, Liu J. The yak genome and adaptation to life at high altitude. Nat Genet. 2012;44(8):946–9.
50. Aunins AW, Nelms DL, Hobson CS, King TL. Comparative mitogenomic analyses of three north American stygobiont amphipods of the genus *Stygobromus* (Crustacea: Amphipoda). Mitochondrial DNA Part B. 2016;1(1):560–3.
51. Benito JB, Porter ML, Niemiller ML. The mitochondrial genomes of five spring and groundwater amphipods of the family Crangonyctidae (Crustacea: Amphipoda) from eastern North America. Mitochondrial DNA B. 2021;6(6):1662–7.
52. Andrews S. FastQC: a quality control tool for high throughput sequence data. 2010. Available online at: http://www.bioinformatics.babraham.ac.uk/projects/fastqc.
53. Bolger AM, Lohse M, Usadel B. Trimmomatic: a flexible trimmer for Illumina sequence data. Bioinf (Oxford England). 2014;30(15):2114–20.
54. Das J. The role of mitochondrial respiration in physiological and evolutionary adaptation. BioEssays. 2006;28(9):890–901.
55. Bernt M, Donath A, Jühling F, Externbrink F, Florentz C, Fritzsch G, Pütz M, Middendorf M, Stadler PF. MITOS: improved de novo metazoan mitochondrial genome annotation. Mol Phylogenet Evol. 2013;69:313–9.
56. Juan C, Guzik MT, Jaume D, Cooper SJ. Evolution in caves: Darwin's 'wrecks of ancient life'in the molecular era. Mol Ecol. 2010;19(18):3865–80.
57. Wheeler DL, Church DM, Federhen S, Lash AE, Madden TL, Pontius JU, Schuler GD, Schriml LM, Sequeira E, Tatusova TA, Wagner L. Database resources of the National Center for Biotechnology. Nucleic Acids Res. 2003;31(1):28–33.
58. Zhang D, Li WX, Zou H, Wu SG, Li M, Jakovlić I, Wang GT. Mitochondrial genomes of two diplectanids (Platyhelminthes: Monogenea) expose paraphyly of the order Dactylogyridea and extensive tRNA gene rearrangements. Parasites Vectors. 2018;11(1):1–13.

59. Zhang D, Gao F, Jakovlić I, Zou H, Zhang J, Li WX, Wang GT. PhyloSuite: an integrated and scalable desktop platform for streamlined molecular sequence data management and evolutionary phylogenetics studies. Mol Ecol Resour. 2020;20(1):348–55.
60. Bernt M, Merkle D, Ramsch K, Fritzsch G, Perseke M, Bernhard D, Middendorf M. CREx: inferring genomic rearrangements based on common intervals. Bioinformatics. 2007;23(21):2957–8.
61. Lessinger AC, Junqueira M, Lemos AC, Kemper TA, Silva ELD, Vettore FR, Arruda ALP, Azeredo-Espin LAM. The mitochondrial genome of the primary screwworm fly *Cochliomyia hominivorax* (Diptera: Calliphoridae). Insect Mol Biol. 2000;9(5):521–9.
62. Qu Y, Zhao H, Han N, Zhou G, Song G, Gao B, Lei F. Ground tit genome reveals avian adaptation to living at high altitudes in the tibetan plateau. Nat Commun. 2013;4(1):1–9.
63. Jühling F, Pütz J, Bernt M, Donath A, Middendorf M, Florentz C, Stadler PF. Improved systematic tRNA gene annotation allows new insights into the evolution of mitochondrial tRNA structures and into the mechanisms of mitochondrial genome rearrangements. Nucleic Acids Res. 2012;40(7):2833–45.
64. Castresana J. Selection of conserved blocks from multiple alignments for their use in phylogenetic analysis. Mol Biol Evol. 2000;17(4):540–52.
65. Krebes L, Bastrop R. The mitogenome of *Gammarus duebeni* (Crustacea Amphipoda): a new gene order and non-neutral sequence evolution of tandem repeats in the control region. Comp Biochem Physiol D Genomics Proteomics. 2012;7(2):201–11.
66. Ronquist F, Teslenko M, van der Mark P, Ayres DL, Darling A, Höhna S, Larget B, Liu L, Suchard MA, Huelsenbeck JP. MrBayes 3.2: efficient bayesian phylogenetic inference and model choice across a large model space. Syst Biol. 2012;61:539–42.
67. Rambaut A, Drummond AJ, Xie D, Baele G, Suchard MA. Posterior summarization in bayesian phylogenetics using Tracer 1.7. Syst Biol. 2018;67(5):901.
68. Xu B, Yang Z. PAMLX: a graphical user interface for PAML. Mol Biol Evol. 2013;30(12):2723–4.
69. Yang L, Wang Y, Zhang Z, He S. Comprehensive transcriptome analysis reveals accelerated genic evolution in a Tibet fish, *Gymnodiptychus pachycheilus*. Genome Biol Evol. 2015;7(1):251–61.
70. Engel AS, Porter ML, Stern LA, Quinlan S, Bennett PC. Bacterial diversity and ecosystem function of filamentous microbial mats from aphotic (cave) sulfidic springs dominated by chemolithoautotrophic Epsilonproteobacteria. FEMS Microbiol Ecol. 2004;51(1):31–53.
71. Weaver S, Shank SD, Spielman SJ, Li M, Muse SV, Pond K, S. L. Datamonkey 2.0: a modern web application for characterizing selective and other evolutionary processes. Mol Biol Evol. 2018;35(3):773–7.
72. Smith MD, Wertheim JO, Weaver S, Murrell B, Scheffler K, Pond K, S. L. Less is more: an adaptive branch-site random effects model for efficient detection of episodic diversifying selection. Mol Biol Evol. 2015;32(5):1342–53.
73. Mu W, Liu J, Zhang H. Complete mitochondrial genome of *Benthodytes marianensis* (Holothuroidea: Elasipodida: Psychropotidae): Insight into deep sea adaptation in the sea cucumber. PLoS One. 2018;13(11):e0208051.
74. Wertheim JO, Murrell B, Smith MD, Pond K, S. L., Scheffler K. RELAX: detecting relaxed selection in a phylogenetic framework. Mol Biol Evol. 2015;32(3):820–32.
75. Clary DO, Wolstenholme DR. The mitochondrial DNA molecule of *Drosophila yakuba*: nucleotide sequence, gene organization, and genetic code. J Mol Evol. 1985;22(3):252–71.
76. Romanova EV, Aleoshin VV, Kamaltynov RM, Mikhailov KV, Logacheva MD, Sirotinina EA, Sherbakov DY. Evolution of mitochondrial genomes in Baikalian amphipods. BMC Genomics. 2016;17(14):291–306.
77. Bauzà-Ribot MM, Jaume D, Juan C, Pons J. The complete mitochondrial genome of the subterranean crustacean *Metacrangonyx longipes* (Amphipoda): a unique gene order and extremely short control region: full-length Research Paper. Mitochondrial DNA. 2009;20(4):88–99.
78. Ki JS, Hop H, Kim SJ, Kim IC, Park HG, Lee JS. Complete mitochondrial genome sequence of the Arctic gammarid, *Onisimus nanseni* (Crustacea; Amphipoda): novel gene structures and unusual control region features. Comp Biochem Physiol D Genomics Proteomics. 2010;5(2):105–15.
79. Issartel J, Voituron Y, Guillaume O, Clobert J, Hervant F. Selection of physiological and metabolic adaptations to food deprivation in the Pyrenean newt *Calotriton asper* during cave colonisation. Comp Biochem Physiol A Mol Integr Physiol. 2010;155(1):77–83.
80. Rivarola-Duarte L, Otto C, Jühling F, Schreiber S, Bedulina D, Jakob L, Stadler PF. A first glimpse at the genome of the Baikalian amphipod *Eulimnogammarus verrucosus*. J Exp Zool Mol Dev Evol. 2014;322(3):177–89.
81. Kornobis E, Pálsson SN, Svavarsson J. Classification of *Crangonyx Islandicus* (Amphipoda, Crangonyctidae) based on morphological characters and comparison with molecular phylogenies. Zootaxa. 2012;3233(1):52–66.
82. Macey JR, Larson A, Ananjeva NB, Papenfuss TJ. Replication slippage may cause parallel evolution in the secondary structures of mitochondrial transfer RNAs. Mol Biol Evol. 1997;14(1):30–9.
83. Katoh K, Standley DM. MAFFT multiple sequence alignment software version 7: improvements in performance and usability. Mol Biol Evol. 2013;30(4):772–80.
84. Shin SC, Cho J, Lee JK, Ahn DH, Lee H, Park H. Complete mitochondrial genome of the Antarctic Amphipod *Gondogeneia Antarctica* (Crustacea, amphipod). Mitochondrial DNA. 2012;23(1):25–7.
85. Yang HM, Song JH, Kim MS, Min GS. The complete mitochondrial genomes of two talitrid amphipods, Platorchestia Japonica and P. Parapacifica (Crustacea, Amphipoda). Mitochondrial DNA B. 2017;2(2):757–8.
86. R Core Team.. R: A language and environment for statistical computing. R Foundation for Statistical Computing, Vienna, Austria. 2021. https://www.R-project.org/.
87. Dierckxsens N, Mardulyn P, Smits G. NOVOPlasty: de novo assembly of organelle genomes from whole genome data. Nucleic Acids Res. 2017;45(4):e18–8.
88. Reyes A, Gissi C, Pesole G, Saccone C. Asymmetrical directional mutation pressure in the mitochondrial genome of mammals. Mol Biol Evol. 1998;15(8):957–66.
89. Wei SJ, Shi M, Chen XX, Sharkey MJ, van Achterberg C, Ye GY, He JH. New views on strand asymmetry in insect mitochondrial genomes. PLoS One. 2010;5(9):e12708.
90. Hao YJ, Zou YL, Ding YR, Xu WY, Yan ZT, Li XD, Chen B. Complete mitochondrial genomes of Anopheles stephensi and an. Dirus and comparative evolutionary mitochondriomics of 50 mosquitoes. Sci Rep. 2017;7(1):1–13.
91. Zhang J, Nielsen R, Yang Z. Evaluation of an improved branch-site likelihood method for detecting positive selection at the molecular level. Mol Biol Evol. 2005;22(12):2472–9.
92. Peng Y, Yang Z, Zhang H, Cui C, Qi X, Luo X, Su B. Genetic variations in tibetan populations and high-altitude adaptation at the Himalayas. Mol Biol Evol. 2011;28(2):1075–81.
93. Macher JN, Leese F, Weigand AM, Rozenberg A. The complete mitochondrial genome of a cryptic amphipod species from the Gammarus fossarum complex. Mitochondrial DNA Part B. 2017;2(1):17–8.
94. Rawlings TA, Collins TM, Bieler R. A major mitochondrial gene rearrangement among closely related species. Mol Biol Evol. 2001;18(8):1604–9.
95. Zou H, Jakovlić I, Chen R, Zhang D, Zhang J, Li WX, Wang GT. The complete mitochondrial genome of parasitic nematode *Camallanus cotti*: extreme discontinuity in the rate of mitogenomic architecture evolution within the Chromadorea class. BMC Genomics. 2017;18(1):1–17.
96. Boore JL, Macey JR, Medina M. Sequencing and comparing whole mitochondrial genomes of animals. Methods Enzymol. 2005;395:311–48.
97. Lanfear R, Calcott B, Ho SY, Guindon S. PartitionFinder: combined selection of partitioning schemes and substitution models for phylogenetic analyses. Mol Biol Evol. 2012;29(6):1695–701.
98. Castresana J, Feldmaier-Fuchs G, Pääbo S. Codon reassignment and amino acid composition in hemichordate mitochondria. Proc Natl Acad Sci. 1998;95(7):3703–7.
99. Nair P, Huertas M, Nowlin WH. Metabolic responses to long-term food deprivation in subterranean and surface amphipods. Subterr Biol. 2020;33:1–15.
100. Niemiller ML, Porter ML, Keany J, Gilbert H, Fong DW, Culver DC, Taylor SJ. Evaluation of eDNA for groundwater invertebrate detection and monitoring: a case study with endangered *Stygobromus* (Amphipoda: Crangonyctidae). Conserv Genet Resour. 2018;10(2):247–57.

101. Wilson K, Cahill V, Ballment E, Benzie J. The complete sequence of the mitochondrial genome of the crustacean *Penaeus monodon*: are malacostracan crustaceans more closely related to insects than to branchiopods? Mol Biol Evol. 2000;17(6):863–74.
102. Ren J, Shen X, Jiang F, Liu B. The mitochondrial genomes of two scallops, *Argopecten irradians* and *Chlamys farreri* (Mollusca: Bivalvia): the most highly rearranged gene order in the family Pectinidae. J Mol Evol. 2010;70(1):57–68.
103. Ren J, Liu X, Jiang F, Guo X, Liu B. Unusual conservation of mitochondrial gene order in *Crassostrea* oysters: evidence for recent speciation in Asia. BMC Evol Biol. 2010a;10(1):1–14.
104. Xin Y, Ren J, Liu X. Mitogenome of the small abalone *Haliotis diversicolor* Reeve and phylogenetic analysis within Gastropoda. Mar Genom. 2011;4(4):253–62.
105. Bauzà-Ribot MM, Juan C, Nardi F, Oromí P, Pons J, Jaume D. Mitogenomic phylogenetic analysis supports continental-scale vicariance in subterranean thalassoid crustaceans. Curr Biol. 2012;22(21):2069–74.
106. Li XD, Jiang GF, Yan LY, Li R, Mu Y, Deng WA. Positive selection drove the adaptation of mitochondrial genes to the demands of flight and high-altitude environments in grasshoppers. Front Genet. 2018;9:605.
107. Ojala D, Montoya J, Attardi G. tRNA punctuation model of RNA processing in human mitochondria. Nature. 1981;290(5806):470–4.
108. Lin FJ, Liu Y, Sha Z, Tsang LM, Chu KH, Chan TY, Cui Z. Evolution and phylogeny of the mud shrimps (Crustacea: Decapoda) revealed from complete mitochondrial genomes. BMC Genomics. 2012;13(1):1–12.
109. Yamazaki N, Ueshima R, Terrett JA, Yokobori SI, Kaifu M, Segawa R, Thomas RH. Evolution of pulmonate gastropod mitochondrial genomes: comparisons of gene organizations of Euhadra, Cepaeaand Albinaria and implications of unusual tRNA secondary structures. Genetics. 1997;145(3):749–58.
110. Nardi F, Carapelli A, Fanciulli PP, Dallai R, Frati F. The complete mitochondrial DNA sequence of the basal hexapod *Tetrodontophora bielanensis*: evidence for heteroplasmy and tRNA translocations. Mol Biol Evol. 2001;18(7):1293–304.
111. Copilaş-Ciocianu D, Sidorov D, Gontcharov A. Adrift across tectonic plates: molecular phylogenetics supports the ancient laurasian origin of old limnic crangonyctid amphipods. Org Divers Evol. 2019;19:191–207.
112. Kilpert F, Podsiadlowski L. The mitochondrial genome of the Japanese skeleton shrimp Caprella mutica (Amphipoda: Caprellidea) reveals a unique gene order and shared apomorphic translocations with Gammaridea. Mitochondrial DNA. 2010;21(3–4):77–86.
113. Koenemann S, Holsinger JR. Systematics of the north American subterranean amphipod genus *Bactrurus*. (Crangonyctidae) Beaufortia. 2001;51(1):1–56.
114. Kornobis E, Pálsson S, Sidorov DA, Holsinger JR, Kristjánsson BK. Molecular taxonomy and phylogenetic affinities of two groundwater amphipods, *Crangonyx islandicus* and *Crymostygius Thingvallensis*, endemic to Iceland. Mol Phylogenet Evol. 2011;58(3):527–39.
115. Carroll J, Fearnley IM, Wang Q, Walker JE. Measurement of the molecular masses of hydrophilic and hydrophobic subunits of ATP synthase and complex I in a single experiment. Anal Biochem. 2009;395(2):249–55.
116. Matsumoto Y, Yanase T, Tsuda T, Noda H. Species–specific mitochondrial gene rearrangements in biting midges and vector species identification. Med Vet Entomol. 2009;23(1):47–55.
117. Scheffler IE. Molecular genetics of succinate: quinone oxidoreductase in eukaryotes. Prog Nucl Acid Res Mol Biol. 1998;60:267–315.
118. Guo H, Yang H, Tao Y, Tang D, Wu Q, Wang Z, Tang B. Mitochondrial OXPHOS genes provides insights into genetics basis of hypoxia adaptation in anchialine cave shrimps. Genes Genomics. 2018;40(11):1169–80.
119. McKenzie M, Lazarou M, Ryan MT. Analysis of respiratory chain complex assembly with radiolabeled nuclear- and mitochondrial-encoded subunits. Methods Enzymol. 2009;456:321–39.
120. Zapelloni F, Jurado-Rivera JA, Jaume D, Juan C, Pons J. Comparative Mitogenomics in *Hyalella* (Amphipoda: Crustacea). Genes. 2021;12(2):292.
121. Meiklejohn CD, Montooth KL, Rand DM. Positive and negative selection on the mitochondrial genome. Trends Genet. 2007;23(6):259–63.
122. Mitterboeck TF, Adamowicz SJ. Flight loss linked to faster molecular evolution in insects. Proc Royal Soc Biol Sci. 2013;280(1767):20131128.
123. Zhang H, Luo Q, Sun J, Liu F, Wu G, Yu J, Wang W. Mitochondrial genome sequences of *Artemia tibetiana* and *Artemia urmiana*: assessing molecular changes for high plateau adaptation. Sci China Life Sci. 2013a;56(5):440–52.
124. Taylor SJ, Niemiller ML. Biogeography and conservation assessment of *Bactrurus* groundwater amphipods (Crangonyctidae) in the central and eastern United States. Subterr Biol. 2016;17:1–29.
125. Hassanin A, Leger NELLY, Deutsch J. Evidence for multiple reversals of asymmetric mutational constraints during the evolution of the mitochondrial genome of Metazoa, and consequences for phylogenetic inferences. Syst Biol. 2005;54(2):277–98.
126. Carlini DB, Fong DW. The transcriptomes of cave and surface populations of *Gammarus minus* (Crustacea: Amphipoda) provide evidence for positive selection on cave downregulated transcripts. PLoS One. 2017;12(10):e0186173.
127. Garvin MR, Bielawski JP, Gharrett AJ. Positive Darwinian selection in the piston that powers proton pumps in complex I of the mitochondria of Pacific salmon. PLoS One. 2011;6(9):e24127.
128. Zhang D, Zou H, Hua CJ, Li WX, Mahboob S, Al-Ghanim KA, Wang GT. Mitochondrial architecture rearrangements produce asymmetrical nonadaptive mutational pressures that subvert the phylogenetic reconstruction in Isopoda. Genome Biol Evol. 2019;11(7):1797–812.
129. Okimoto R, Wolstenholme DR. A set of tRNAs that lack either the T psi C arm or the dihydrouridine arm: towards a minimal tRNA adaptor. EMBO J. 1990;9(10):3405–11.
130. Xiao JH, Jia JG, Murphy RW, Huang DW. Rapid evolution of the mitochondrial genome in chalcidoid wasps (Hymenoptera: Chalcidoidea) driven by parasitic lifestyles. PLoS One. 2011;6(11):e26645.
131. Wirth C, Brandt U, Hunte C, Zickermann V. Structure and function of mitochondrial complex I. Biochim et Biophys Acta (BBA)-Bioenergetics. 2016;1857(7):902–14.
132. Dowling TE, Martasian DP, Jeffery WR. Evidence for multiple genetic forms with similar eyeless phenotypes in the blind cavefish, *Astyanax mexicanus*. Mol Biol Evol. 2002;19(4):446–55.
133. Zhang ZY, Chen B, Zhao DJ, Kang L. Functional modulation of mitochondrial cytochrome c oxidase underlies adaptation to high-altitude hypoxia in a Tibetan migratory locust. Proc Royal Soc B Biol Sci. 2013;280(1756):20122758.

Publisher's Note